



UNIVERSITEIT•STELLENBOSCH•UNIVERSITY  
jou kennisvennoot • your knowledge partner

# A Critical Analysis of Design Flaws in the Death Star

Luke Skywalker  
99652154

Report submitted in partial fulfilment of the requirements of the module  
Project (E) 448 for the degree Baccalaureus in Engineering in the Department of  
Electrical and Electronic Engineering at Stellenbosch University.

Supervisor: Dr O. W. Kenobi

October 2099

# **Acknowledgements**

I would like to thank my dog, Muffin. I also would like to thank the inventor of the incubator; without him/her, I would not be here. Finally, I would like to thank Dr Herman Kamper for this amazing report template.



UNIVERSITEIT•STELLENBOSCH•UNIVERSITY  
jou kennisvennoot • your knowledge partner

## Plagiaatverklaring / Plagiarism Declaration

1. Plagiaat is die oorneem en gebruik van die idees, materiaal en ander intellektuele eiendom van ander persone asof dit jou eie werk is.

*Plagiarism is the use of ideas, material and other intellectual property of another's work and to present it as my own.*

2. Ek erken dat die pleeg van plagiaat 'n strafbare oortreding is aangesien dit 'n vorm van diefstal is.

*I agree that plagiarism is a punishable offence because it constitutes theft.*

3. Ek verstaan ook dat direkte vertalings plagiaat is.

*I also understand that direct translations are plagiarism.*

4. Dienooreenkomsdig is alle aanhalings en bydraes vanuit enige bron (ingesluit die internet) volledig verwys (erken). Ek erken dat die woordelikse aanhaal van teks sonder aanhalingstekens (selfs al word die bron volledig erken) plagiaat is.

*Accordingly all quotations and contributions from any source whatsoever (including the internet) have been cited fully. I understand that the reproduction of text without quotation marks (even when the source is cited) is plagiarism*

5. Ek verklaar dat die werk in hierdie skryfstuk vervat, behalwe waar anders aangedui, my eie oorspronklike werk is en dat ek dit nie vantevore in die geheel of gedeeltelik ingehandig het vir bepunting in hierdie module/werkstuk of 'n ander module/werkstuk nie.

*I declare that the work contained in this assignment, except where otherwise stated, is my original work and that I have not previously (in its entirety or in part) submitted it for grading in this module/assignment or another module/assignment.*

Studentenommer / Student number	Handtekening / Signature
Voorletters en van / Initials and surname	Datum / Date

# **Abstract**

## **English**

The English abstract.

# **Contents**

# **List of Figures**

# **List of Tables**

# Nomenclature

## Acronyms and abbreviations

<i>USV</i>	Unmanned Sailing Vessel.
<i>GPS</i>	Global Positioning System.
<i>RC</i>	Radio Controlled
<i>CAD</i>	Computer Aided Design
<i>Pcontroller</i>	Proportional controller
<i>PI</i>	Proportional Integral
<i>PID</i>	Proportional Integral Derivative
<i>FPGA</i>	Field Programmable Gate Array
<i>SPI</i>	Serial Peripheral Interface
<i>IMU</i>	Inertial Measurement Unit
<i>PWM</i>	Pulse Width Modulation
<i>NMEA</i>	
<i>ASCII</i>	American Standard Character for Information and Interchange
<i>ADC</i>	Analog to Digital Converter
<i>UART</i>	
<i>PWM</i>	Pulse Width Modulation
<i>FAT32</i>	File Allocation Table, 32 bits
<i>LSB</i>	Least Significant Bit
<i>LPF</i>	Low Pass Filter
<i>PCB</i>	Printed Circuit Board

# **Chapter 1**

## **Introduction**

### **1.1. Background**

The ocean covers 71% of the earth's surface and 80% of it remains unmapped, unobserved, and unexplored. The ocean produces over half of the air we breathe and absorbs 50 times more carbon dioxide than our atmosphere currently does. It regulates our climate and the weather patterns by transporting heat from the equator to the poles. It provides sustenance to millions of people around the world. Without the ocean, life as we know it would not be possible and the planet would become uninhabitable. With that being said the rapidly growing global population and consequent resource consumption is impacting the global environment on a scale that has never been seen before.

Ocean research has led to our current understanding of the huge role the oceans play in supporting life on this planet. The continuing research and exploration of our oceans will aid in assessing the growing negative impact human activity has on the oceans, and by better understanding this impact, more effective solutions can be developed. Ocean research requires large amounts of funding and human resources to support it. As of 2015 the United States had 4000 ocean science researchers, roughly 50 nationally maintained ocean research vessels and in 2013 had an annual national ocean science expenditure of \$12.5 trillion [?]. These ocean research vessel cost from \$10000 to \$40000 a day to operate, with the crew itself being one of the biggest expenses [?]. These expenses can increase greatly when research missions to remote areas of the globe are conducted, many of these areas being hard or even impossible to access via research vessels.

Advancements in robotics and the development of unmanned vehicles can help bring down the cost and complexity associated with ocean research missions as well as increase the quality of research done. Unmanned sailing vessels(USV) will be able to travel long distances over the ocean, for long periods of time, to remote and inaccessible locations and with little power consumption. USV's can be equipped with various high quality sensors such as hydrophones that are used in marine research. The integration of solar panels with USV's can further increase the range and duration they are capable of.

## 1.2. Problem Statement

To design and develop the navigational and control systems for an unmanned sailing vessel that will enable it to sail along a predetermined route with a relative degree of accuracy. The route to be travelled is defined by a set of GPS coordinates.

## 1.3. Objectives

This section will state the objectives that need to be achieved in order to address the problem statement.

1. Design and develop a digital compass that compensates for tilt.
2. Determine and compare the accuracy of heading obtained from a GPS receiver and that from a digital compass.
3. System must be capable of logging operational data to a micro-SD card.
4. Design and develop sail control system.
5. Design and develop rudder control system.
6. Design and implement necessary navigational algorithms: Determine distance and bearing between two GPS coordinate.
7. Design and develop software that ensures system is capable of navigating to predetermined waypoints.
8. Design and implement tacking manouvre into system.

## 1.4. Summary of Work

## 1.5. Scope

## 1.6. Report Overview

# Chapter 2

## Literature

### 2.1. Sail Theory

This section covers the sailing theory that is required for the sections that follow, and is taken from the official manual of the american sailing association [?]. Fig. ?? illustrates the anatomy of a typical sailboat. The anatomy of a sailboat is as follows:

- Hull: Watertight floating body of the sailboat that gives it form and supports all parts of the part.
- Keel: Fixed fin on the underside of the sailboat that provides sideways resistance needed to counter the force of the wind on the sails.
- Stern: The back-end of the sailboat.
- Bow: The front-end of the sailboat
- Starboard: When standing at the stern, facing the bow, starboard is the right side of the boat.
- Port: When standing at the stern, facing the bow, port is the left side of the boat
- Rudder: Fin located beneath the stern. The angle of the rudder is adjusted to steer the direction of the sailboat.
- Helm: The mechanism by which the rudder angle is adjusted.
- Mast: Vertical beam attached to the hull which houses the mainsail
- Mainsail: Sail that attaches to the mast of the sailboat.
- Jib: sail that attaches to the bow and the top of the mast.

When on a sailboat the direction of the wind relative to the boat is known as the apparent wind, the direction of the wind relative to a fixed point - a point that has a zero velocity - is known as true wind. When the sailboat has a velocity that is not zero -

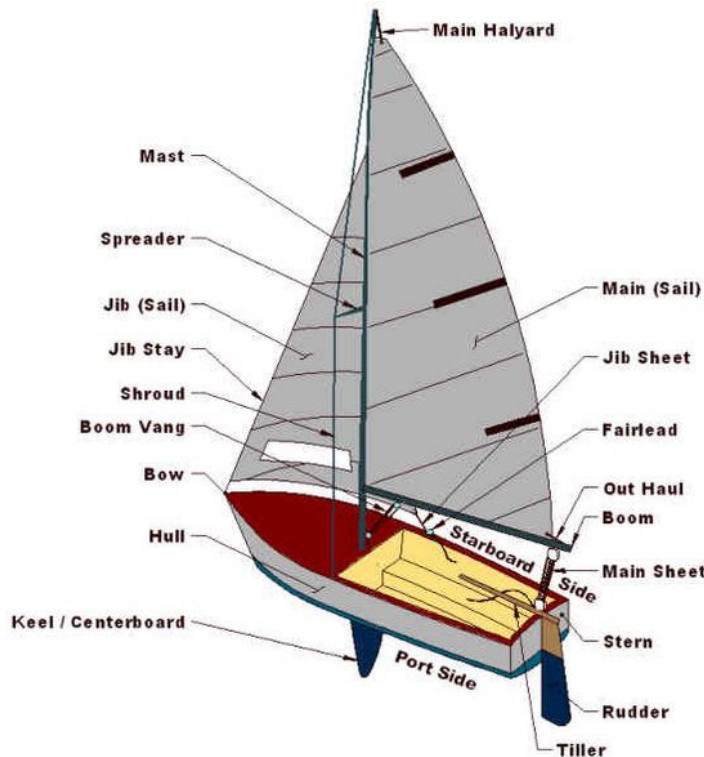


**Figure 2.1:** Sailboat anatomy [?]

sailboat not standing still - the apparent wind has a velocity that differs from the velocity of true wind. Fig. ?? illustrates this concept.

The sail of a sailboat acts similar to that of an airplane wing - it produces lift when orientated correctly. It is this lift that propels the sailboat forward. The orientation of the sail relative to the apparent wind therefore determines how much force is applied to the boat, any component of this force that acts perpendicular to the centerline of the boat is canceled by the opposing force of the water on the keel. The act of changing the orientation of the sails is known as 'trimming the sails'. To generate a maximum amount of forward force on the sailboat, the sail must be positioned to capture as much of the wind's energy as possible. The direction of apparent wind determines the directions that

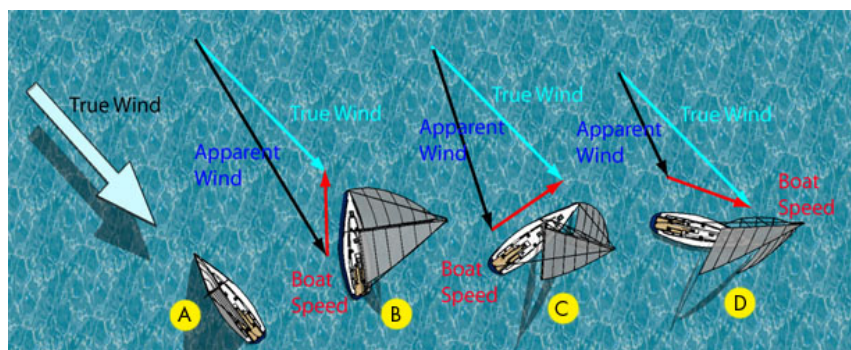


**Figure 2.2:** Apparent wind [?]

the sailboat can/cannot sail, these directions are known as points of sail and are measured relative to the direction of apparent wind. Fig. ?? illustrates the points of sail of a sailboat. It should be noted that there is a range known as the 'no-sail zone' in which a sailboat cannot sail. This range is measured  $45^\circ$  to both sides of the apparent wind when sailing directly towards the apparent wind.

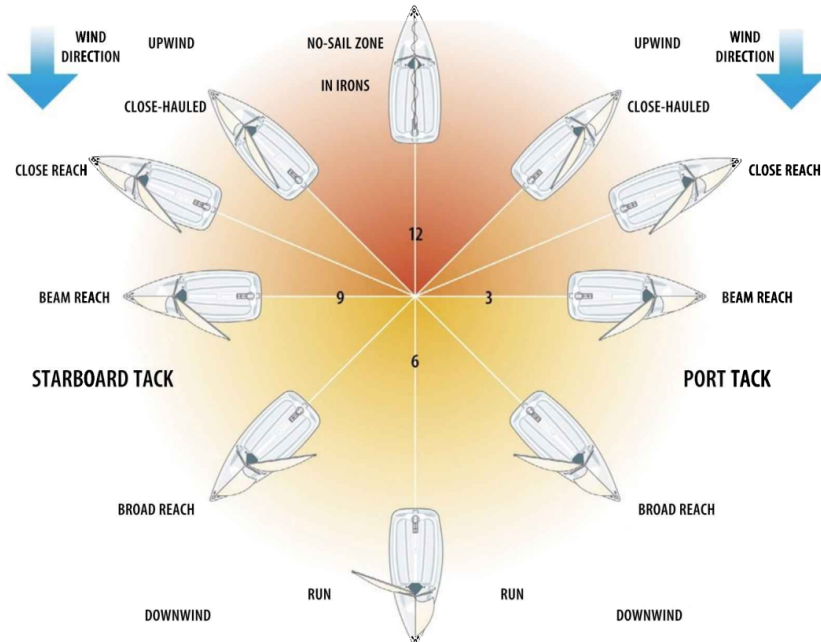


**Figure 2.3:** Point of sail [?]

Point of sail is traditionally measured analogous to a clock, as shown in Fig. ???. For the purpose of this report point of sail will be defined as the angle between apparent wind direction and the direction of travel of the boat, measured clockwise in degrees. A sail direction of  $0^\circ$  will then correspond to 12'o'clock in Fig.?? and  $180^\circ$  will correspond to 6'o'clock measured clockwise. The position of the mainsail will be defined by the angle between the mainsail and the centerline of the sailboat to either the starboard or port side.

If the desired destination is within the no-sail zone, a manoeuvre known as 'tacking' can be performed to reach the desired destination. When sailing with the wind blowing on the starboard, it's on the starboard tack, and when the wind is blowing on port side, the boat is on port tack. Tacking is the act of turning the bow of the sailboat through the no-sail zone. Assume the boat is on starboard tack and point of sail is  $45^\circ$ , after some distance has been travelled the bow is turned through the no-sail zone to attain a port tack and a point of sail of  $-45^\circ$ , this 'zig-zag' motion is done continuously until the desired destination is reached.

Another important manoeuvre is the 'jibe', which is defined as the action of changing from a starboard tack to a port tack. An example of this occurring is when point of sail changes from  $160^\circ$  to  $100^\circ$ , initially apparent wind will be port side but after crossing over  $180^\circ$  the wind will be starboard side, during this crossover the mainsail will often swing

from starboard to port.

## 2.2. Related Work

### 2.2.1. Unmanned Sailing Vessel by Philip van Schalkwyk

Philip is a mechatronics graduate who designed and developed an unmanned sailing vessel for his final year project at Stellenbosch University [?].

#### Objectives

The purpose of the project was to design and develop an USV that is capable of semi-autonomous sailing. The objectives are as follows:

- Design and develop a low-cost digital compass that produces accurate readings with tilt compensation.
- Design and develop a low-cost mechanical wind vane that consists of a digital compass for wind direction sensing.
- Retrofit a RC sailing vessel with a micro-controller, digital compass, wind direction sensor, GPS unit and micro-SD card.
- Design and implement navigational and control systems to enable autonomous sailing.

#### Method Used

A RC sailing vessel was retrofitted with a micro-controller that would read data from sensors and adjust the rudder and sail position in order to sail along a desired path. The system consisted of a micro-controller, GPS receiver, a micro-SD card, a digital compass, wind direction sensor and two servo motors - one to control the sail and one to control the rudder angle. The micro-controller that was used was an Espressif ESP-WROOM-32 micro-controller which is relatively low cost and has a 240 MHz clock speed. The electronic compass was used to determine the current bearing of the vessel, it was designed and developed using a magnetometer, accelerometer, gyroscope and tilt compensation algorithms. The MPU9250-6500 9-axis sensor module was used for the electronic compass as it consists of a magnetometer, accelerometer and a gyroscope. A mechanical wind vane was designed with CAD software and printed with a 3D printer. The wind vane was fitted with a magnetometer - also the MPU9250-6500 - which was used to determine the bearing of the wind vane and therefore the wind direction. The GPS receiver that was used for the

navigational system was a Neo M8N GPS, it would log positional data to the micro-SD card.

A proportional controller was used to control the rudder position. The desired heading/bearing was calculated using the current GPS coordinates obtained from the GPS receiver and the target GPS coordinates. A sample would then be taken from the electronic compass which would give the current bearing of the vessel, the difference the current bearing and the desired bearing is the error signal. The proportional controller would then determine the rudder angle given this error signal, and the servo motor controlling the rudder would be adjusted accordingly.

The main sail position was determined by the samples taken from the wind direction sensor and the current bearing. Only three point of sail classifications were used for the sail positions : close-hauled, beam-reach and run. This was done to give more time to navigational and rudder control systems. If it was determined that angle of attack was less than 45 deg the vessel would tack into the wind. This was achieved by calculating the bearing to either side of the no-sail zone, the vessel would then sail with one of these bearings for 50 meters and then change to the other bearing. The vessel would alternate along these bearings until the target destination was reached.

## Results

The e-compass was tested against a magnetic compass and the results showed the average error in bearing to be  $5.84^\circ$ , the e-compass did however produce a consistent spike at  $180^\circ$  across multiple tests. Tests that were done with the GPS receiver showed that the positional accuracy of the GPS receiver was sufficient for the navigational system and data-logging. The wind sensor that was developed was unable to provide wind direction data consistently, a possible explanation for this is that the length of the  $I^2C$  connection is too long and therefore the capacitance in the lines caused a low pass filter effect on the signal. In the final tests that were conducted to verify the successful operation of the control systems, the point of sail classification was set to run initially and sail adjustments were not taken throughout the duration of the test - due to the wind sensor not working. The results of the final test showed that the rudder control system was capable of keeping the vessel on a near constant heading, with a maximum absolute error of  $6^\circ$ . This test was conducted between two GPS coordinates and the vessel therefore sailed on a fixed bearing between them. Fig ?? shows the results of this final test.

## Remaining challenges

The rudder control system designed by Phillip was capable of accurately tracking a desired bearing during tests. Proportional integral control could not be implemented due to the consistent error that occurred during the e-compass testing. The USV that was developed

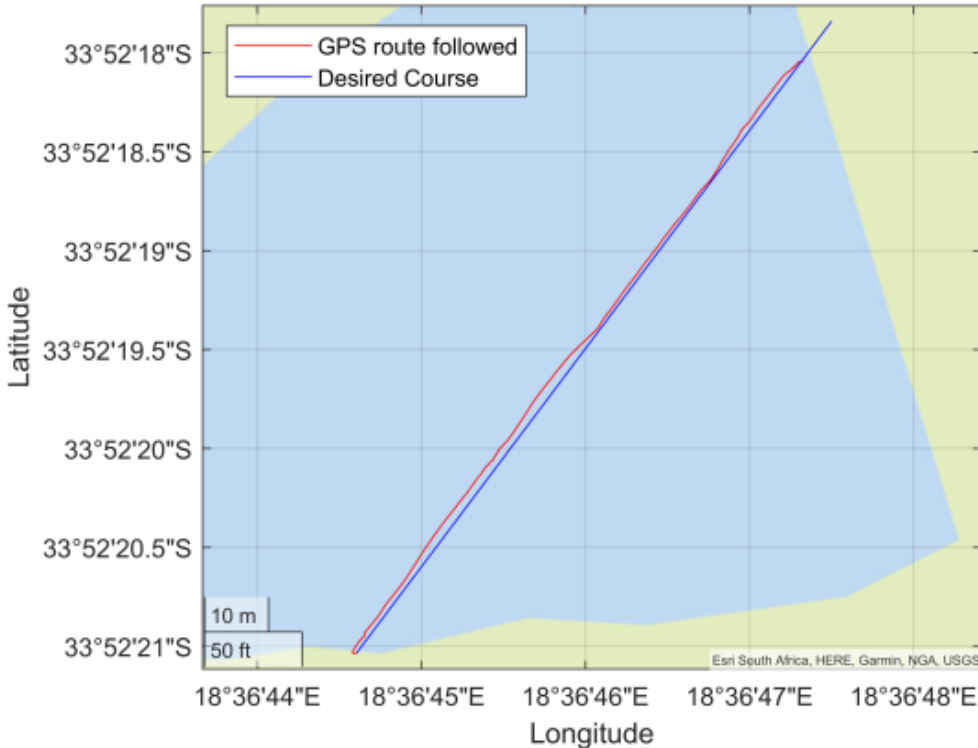


**Figure 2.4:** Test results showing deviation of vessel from ideal trajectory [?]

does not however have the ability to dynamically adjust the sail position according to the relative wind direction, and is therefore unable to achieve the desired performance if wind direction is not constant. Tests were also not conducted to verify the tacking capabilities of USV.

## 2.2.2. Design and Implementation of a Control System for a Sailboat Robot

### Objectives

- Determine the dynamic equations that govern the behavior of a sailboat.
- Use the dynamic equations to design - through simulation- a simple, however effective, controller that can be applied to different types of sail boats.
- Develop a prototype sailboat to implement and test a controller which was designed through simulation.

### Method Used

The system that is developed for an autonomous sailboat consists of two processing units, a combination of sensors, and actuators/servos. Two processing units are used for a

more flexible system. The one processing unit is a ATMega2560 which is built into an arduino, and is used to handle low level control decisions that should be executed in real time. The arduino communicates with the various sensors and implements the control algorithms used to control the actuators in a stable manner. The other processing unit is a Raspberry Pi which is responsible for high level navigation decisions, planning and external communication. The Raspberry Pi is connected to a base station via a XBee radio link of up to 1.6 Km. The two processors communicate with each other via a RS-232 serial connection. The sensors that are used consist of a GPS receiver (EM-406 SiRF III), and a three axis digital compass (actual component used is not specified). A wind sock is used to determine wind direction and this is then transmitted to the system from the base station via XBee. Digital compass is calibrated to compensate for local magnetic declination.

The approach used to design an appropriate control system for an autonomous sailboat is to mathematically model the dynamics of the sailboat, and then through simulation, identify the optimal parameter values of the controller. Determining the dynamics that govern the behavior of a sailboat are divided into calculations of hydrodynamics, moment of inertia, viscous damping, lift, effort sail and centre of mass. These calculations are combined to form Eq. ?? which is used as the control law that governs sailboat control. In Eq. ??  $M_a$  refers to the hydrodynamics,  $C_{rb}$  is dynamics(including centre of mass),  $C_a$  refers to hydrodynamics related to coriolis and centripetal forces,  $D_k$  term is the lift moments generated by the keel and  $D_h$  are the lift forces acting on the hull.

$$(M_{RB} + M_A)\dot{v} = \tau_s + \tau_r - (C_{RB}(v) + C_A(v))v - (D_k(v) + D_h(V))V - g(\eta) \quad (2.1)$$

Two controllers are initially developed: a PID controller for rudder control, and a fuzzy controller, which controls the sail position. By making use of Eq. ?? and simulation software (MATLAB) optimal parameter values are found for the PID controller. This approach is faster than the traditional method of adjusting the parameters, however since the mathematically model does not truly represent the sailboat the parameter values found are used as initial values to be further adjusted through experimentation.

The rudder controller takes in an error signal as its input and outputs the appropriate control signal to the rudder actuator. The error signal is determined as the difference between the actual bearing of the sail vessel and the desired bearing of the sail vessel. Desired bearing is calculated using current GPS location of the vessel and the target GPS location. The actual bearing of the sail boat is determined from the digital compass.

The sail controller takes wind direction as its input and adjusts the sail position accordingly, the controller also takes into account limits of the sail vessel i.e. the dead-zone/no-sail zone.

In the sailboat prototype that is developed, the D parameter used in rudder control is disregarded, mainly because of instability, which is generated due to intensification of high-frequency noise caused by the derivative.

## Results

In the simulation the optimal gains for the rudder controller are:  $K_p = 0.68$ ,  $K_i = 1.125$  and  $K_d = -0.130$ . These controller gains were used as initial values to be fine-tuned through multiple tests done with the prototype sailboat. After conducting the tests the resulting adjusted rudder controller gains were:  $k_p = 2.3$  and  $k_i = 0.8$ . The tests that were done compared the use of a proportional controller and a PI controller for the rudder control, Fig.?? shows the results of one of the tests. Note that the sailboat was initially placed to face  $90^\circ$  from target location. In all tests that were conducted the prototype sailboat reached the specified target coordinates, the PI controller, however, performed better than the P controller with less deviation from the ideal trajectory.

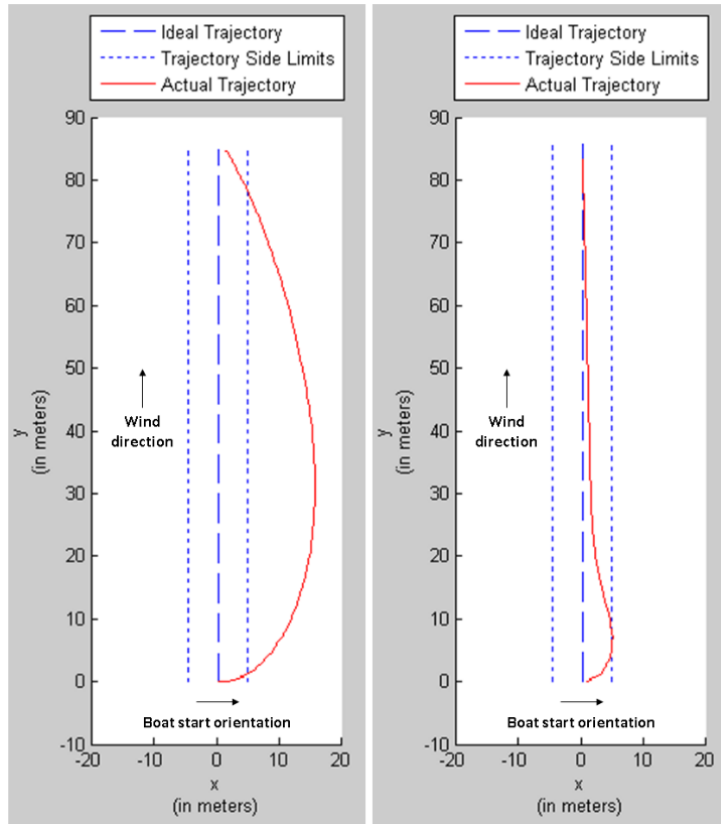


**Figure 2.5:** Test results on water; P controller shown left and PI controller on right [?]

## Remaining challenges

The system that was designed and developed does not incorporate an onboard wind direction sensor but instead receives the wind direction data from a base station via XBee.

The sail vessel will therefore not be capable of travelling distances over which the apparent wind direction around the vessel differs from the wind direction around the base station. Aside from this, the system that was developed addresses the problem statement in section ??; the purpose of the following sections is then to duplicate the above system.

### **2.2.3. FASt - An autonomous sailing platform for oceanographic missions**

the purpose of this project was to design and develope an autonomous sailing boat to enter the Microtransat competition - competition for fully autonomous sailing boats wherein the goal is to cross the atlantic ocean [?].

#### **Objectives**

- Design and construct a high performance and light-weight sailboat of suitable size.
- Design and develope an electronics system that will enable long distance autonomous navigation and control of the sailboat.
- The electronics system must include a communication subsystem for short range and long range communication.
- The electronics system should have a low power consumption and powered by a power source that is recharged via photovoltaic cells.

#### **Method Used**

The sailboat hull shape was inspired by modern racing oceanic yachts and was constructed with fiber glass and epoxy resin. The total length of the sailboat is 2.5 m with a mast height of 3.4 m. It features two independently controlled rudders and two sails which are controlled simultaneously

The electronics system was divided into 5 subsystems: computing, communication, sensors, actuators and power management. The computing system consists of a 32-bit RISC microprocessor running with a maximum clock speed of 50 MHz, ROM memory which holds the bootstrap code and various digital modules that interface the processor with the sensors and actuators. The computing system was implemented using a FPGA, the one that was used was a Suzaki SZ130 which is built around a Xilinx FPGA. The board includes central Microblaze processor running at 50 Mhz, 32 MB of SDRAM, 8 MB of SPI flash memory, a serial interface (RS232) and ethernet port implemented externally to the FPGA. The board has 86 input/output pins available, which connect directly to the FPGA. The computing system runs uCLinux which a version of linux which has been simplified and adapted for embedded applications running processors with no memory

management unit. The advantage of using an FPGA is that many of the processing and interfacing functions of the system can be implemented in custom hardware and therefore are not managed by a micro-processor; this allows the use of a micro-processor that runs at significantly lower clock speeds and thus lower overall power consumption.

The communications subsystem consists of a conventional WiFi router (LinkSys WRT54GC), a GSM modem (Siemens MC35), a IRIDIUM SBD modem (model 9601) and a radio control receiver. The WiFi router is to provide convenient short range communication with a laptop, mainly for the purpose of software development, debug and communication purposes. While at sea missions, the GSM modem and IRIDIUM SBD modem will enable small volume communications to take place. The GSM module enables communications within a range of a few kilometers from shore, the IRIDIUM SBD modem communicates via satellite connection and allows and therefore has a global range. The radio control receiver allows for manual control over the sailboat using a 4 channel proportional control RC transmitter.

Sensors used consist of a wind vane, anemometer, boom position sensor, digital compass (LinkSys WRT54GC), GPS receiver(uBlox RCB-4H), inclinometer, voltage monitors, ambient light sensor, interior temperature and a set of water sensors. The wind vain and boom position sensors were custom built using a magnetometer (Austria Micro Systems AS5040) and are used in the sail position control system. The anemometer is a conventional cup rotor that makes use of a hall effect switch, its main purpose is for data collection and data logging during sea missions. The digital compass and the GPS receiver are used for navigation and data logging purposes. The inclinometer is used to determine heel angle which is used to reef the sails. It should be noted that the sailboat that was developed does not have the ability to adjust the area of the sail i.e. reef, the inclinometer was included for future iterations of the project that possess have this ability. The voltage monitors are used to monitor the voltage of the batteries. The ambient light sensor is used to monitor light intensity which affects the voltage produces by photovoltaic cells. Specific hardware was designed and implemented in the FPGA to interface these sensors with the RISC micro-processor.

The actuators in the system consist of two standard high-power RC servos which provide independent control of the two rudders. The two sails are both controlled simultaneously by a DC geared motor. Although having a low efficiency the DC geared motor is extremely robust, and once position and un-powered the gearbox locks the motors shaft in place. Traditional servo motors consume power in holding a certain shaft position in response to an applied force on the shaft. The use of the DC geared motor is therefore advantageous as sail position is only adjusted when changing course or if a change in wind direction occurs, therefore no power is consumed in keeping the shaft fixed in reaction to the force applied by the wind. A multiplexer was implemented in hardware to select the source data that is routed to the actuators, if a RC connection is established then this data is

selected, otherwise data from the computing system is selected.

The power management system consists of a 45 Wp solar panel (Solara SM160M), two 95 Wh Li-ion batteries, a battery charging circuit and a highly efficient power supply. A wind generator was considered to compliment the photovoltaic cells but ones available commercially are too large and heavy for this application. The total power consumption of the system was measured to be 560 ma.

The software is divided into five modules that implement the five main tasks: hardware interface, helm, sail, skipper and logger. The hardware interface implements all the driver software needed for the processor to communicate with sensors, actuators and configuration parameters. The helm implements the PI controller used to control the rudder position according to wind direction and desired bearing. The commands supported by this module include keeping a fixed bearing, maintaining the angle of apparent wind and performing tacking or gibing maneuvers. The sail module is responsible for controlling the sail position according to wind speed and direction and a set of rules that define best sail angle. This module also implements reefing of the sails - the sheet is eased when heel angle is greater than a certain value. The skipper module sends commands to the helm and sail modules and is responsible for higher level navigation such as deciding what course to follow and when to perform certain sailing maneuvers. The logger module listens to all the other modules and stores relevant data in a log file.

## Results

This article does not cover the testing of the system described above and therefore the validity of the design cannot be verified. The article does however highlight important hardware and software design features to consider when attempting to design an autonomous sailing vessel

## Remaining challenges

The system made use of an FPGA to implement the central computing system as well as interface with the sensors and actuators of the system. While this does decrease the power consumption of the system it also greatly increases the complexity of the design. Many modern micro-controllers already incorporate the hardware needed to interface with the various sensors and actuators used in this system.

Given that the scope of this project stated in section ??, low power consumption of the system, although important in long distance sea missions, is not of vital importance for the purpose of designing and developing the navigational and control systems for an autonomous sail vessel.

The system included functionality that is not needed for the purpose of this project. Some of this functionality includes the simultaneous control of two sails, two rudder

servo's, boom position sensing, wind speed sensing, heel angle sensing, a power supply that incorporates rechargeability and photovoltaic cells, and a communications subsystem for short and long range communication with the vessel.

### 2.2.4. Establishing frame of reference

It is important to establish a fixed frame of reference which can be used to determine the orientation of a vessel at sea. The fixed frame of reference that will be used in this report is the industry standard "NED" (North, East, Down) coordinate system. The NED coordinate system is orientated such that at any position on the earth the x-axis is aligned with true north, the y-axis is aligned with lines of latitude and points east, the z-axis is aligned with the vector that represents the acceleration of gravity. The x,y-plane is therefore tangent to the sphere of the earth. The inertial frame of the sailing vessel is fixed to the body of the sailing vessel and is the perspective that a person on the sailing vessel would have. The x-axis of the inertial frame of the sailing vessel is aligned with the centerline of the vessel and points from the stern to the bow, the y-axis is aligned perpendicular to the centerline of the vessel and points to the starboard side, the z-axis is aligned with the mast of the vessel and points downwards. This concept is illustrated in Fig. ??.

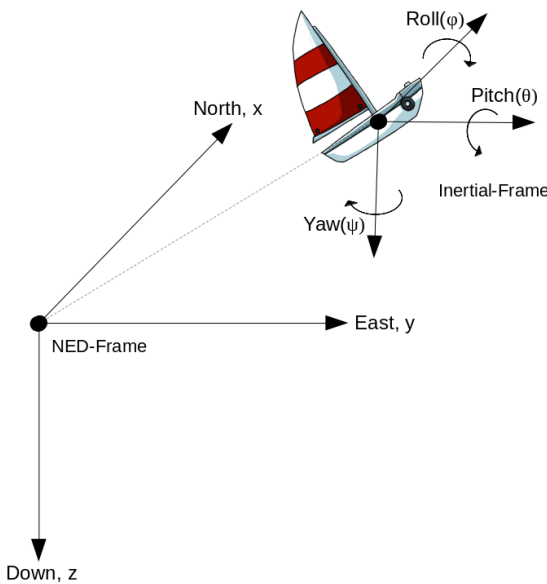


**Figure 2.6:** NED frame of reference

Rotation of the inertial frame about the x-axis is known as the roll angle ( $\phi$ ), rotation about the y-axis is the pitch angle ( $\theta$ ), and rotation about the z-axis is the yaw angle ( $\psi$ ). For all axes, clockwise rotation is taken to be positive rotation. Given that the roll, pitch, and yaw angles are all known it is possible to transform the inertial frame back to the NED frame using transformation matrices in Eq. ??, ??, ?? [?].

$$\mathbf{R}_{x,\phi} = \begin{bmatrix} 1 & 0 & 0 \\ 0 & \cos \phi & -\sin \phi \\ 0 & \sin \phi & \cos \phi \end{bmatrix} \quad (2.2)$$

$$\mathbf{R}_{y,\theta} = \begin{bmatrix} \cos \theta & 0 & \sin \theta \\ 0 & 1 & 0 \\ -\sin \theta & 0 & \cos \theta \end{bmatrix} \quad (2.3)$$

$$\mathbf{R}_{z,\psi} = \begin{bmatrix} \cos \psi & -\sin \psi & 0 \\ \sin \psi & \cos \psi & 0 \\ 0 & 0 & 1 \end{bmatrix} \quad (2.4)$$

### 2.2.5. Magnetic declination

A traditional handheld magnetic compass will align itself with the earth's local magnetic field lines, which in theory run from the magnetic south pole to the magnetic north pole. This means that a magnetic compass will point to magnetic north. However in practice this is not true, the earth's magnetic field lines are not constant, and depending on where measurements are taken there will exist an angle of error. True north is defined as

True north, also known as geographical north, is defined as the point where all lines of longitude intersect. Magnetic north is the point to which a magnetic compass aligns itself, and varies across the globe as well as with time. The direction of magnetic north differs depending location because earth's magnetic field lines do not travel a linear path from magnetic south to magnetic north, this is illustrated in Fig. ??.

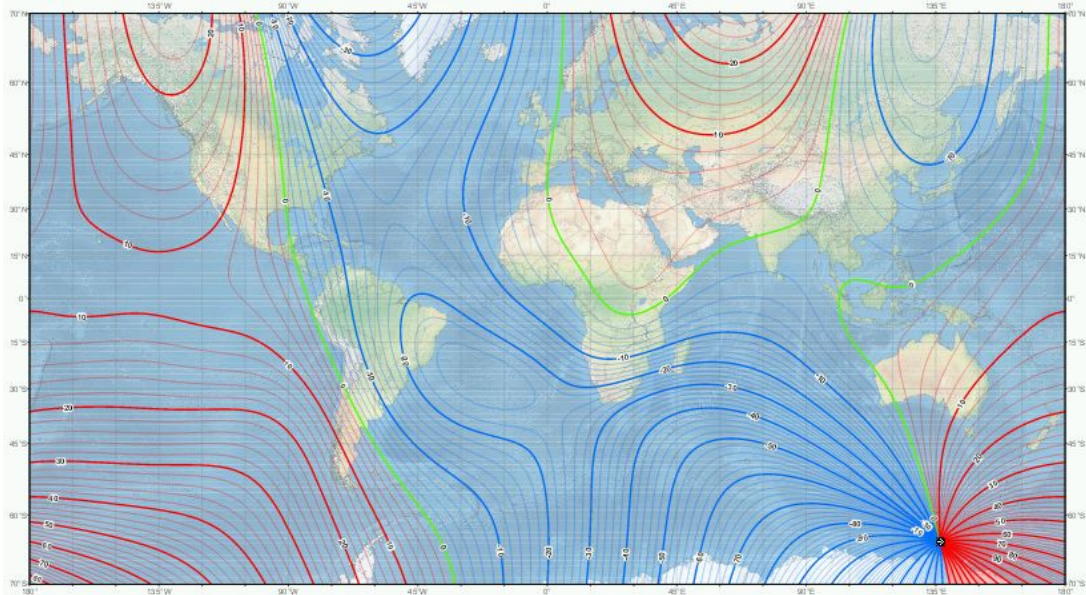


**Figure 2.7:** Magnetic declination across the globe [?]

Magnetic declination is an angle of correction used to determine true north from a

local magnetic north reading. Magnetic declination takes into account the variance of local magnetic field lines and the angle between magnetic north and true north. Magnetic declination therefore differs across the globe. The National Oceanic and Atmospheric Administration (NOAA) keeps track of magnetic declination across the globe as it changes with time. The magnetic declination in Stellenbosch is  $25.77^\circ \pm 0.59^\circ$ .

# Chapter 3

## System Design

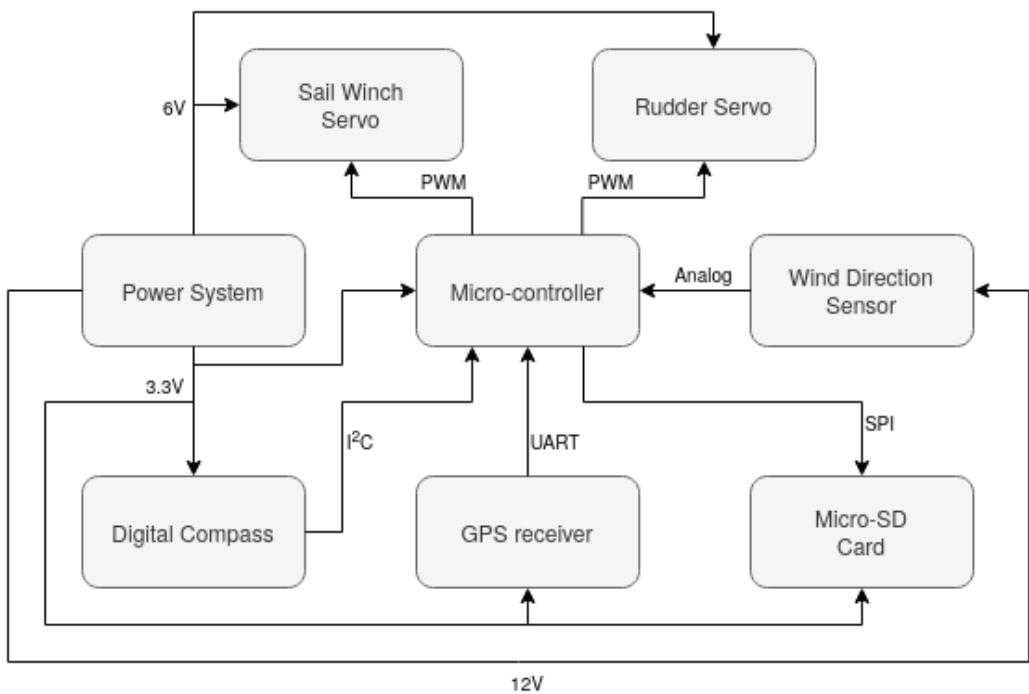


**Figure 3.1:** System Diagram

### 3.1. Sail Vessel

The sailing vessel houses the entire system illustrated in Fig. ???. Designing and developing a sailboat is a complex task on its own, requiring expertise and experience in many fields, some of which include aerodynamics, hydrodynamics and material design. Given the complexity of this task and the time constraints of the project, an existing RC sailboat was used. A Dragonflite 95 RC sailboat [?] was modified to incorporate the system illustrated in Fig. ???. The Dragonflite is 950 mm in length and has an overall weight of two kilograms. It features two sails (mainsail and jib), a carbon fibre mast and moulded carbon fibre keel with zinc alloy ballast bulb. The sailboat is operated with a 2.4Ghz 4-channel digital proportional transmitter which communicates with a 2.4Ghz 4-channel receiver. The

Dragonflite 95 comes preinstalled with a rudder servo motor as well as a sail winch servo motor. The sail winch servo controls both the mainsail and the jib simultaneously. The receiver and two servo motors are powered with a 6v battery source (4 AA batteries). The transmitter and receiver were removed as they are not needed in the development of a autonomous sailboat.

## 3.2. Micro-controller

Two options were considered for the micro-controller: the Adafruit BlackPill STM32F411 development board [?] and a Adafruit STM32F405 Feather [?]. The Adafruit BlackPill has an Arm 32-bit Cortex-M4 CPU, which has a clock speed of 100MHz, 512KB flash memory, 128kB SRAM, and has a power efficiency of  $100\mu A/MHz$ . The Adafruit feather has an Arm 32-bit Cortex-M4 CPU, with a clock speed of 168 MHz, 1MB flash memory, and has a power efficiency of  $238\mu A/MHz$ . Despite the higher price and power consumption of the Adafruit Feather, it was chosen for this system as it has a higher clock speed, which is needed for the navigational and control systems. The Adafruit feather also has a jst connection for a lithium-polymer battery as well as a 3.3V regulator.

## 3.3. Wind direction sensor

The direction of apparent wind is needed to determine the optimal positioning of the sails. Wind direction sensors that were considered where: an ultrasonic anemometer, a mechanical wind vain, and the development of a wind direction sensor using four electret microphones and correlating the signals. The ultrasonic anemometer that was considered was the WS303U by Sentec Meteorology, it was not used because it is too large for the sailing vessel. The development of a wind direction was not done because of the time constraints of the project. The mechanical wind vain was chosen as the most viable option. The sensor used was the FST200-202 [?] made by firstrate sensor company. This sensor is designed for outdoor environments such as weather stations and boats, it therefore has excellent resistance to extreme weather conditions and erosion. The sensor works in wind speeds greater than 0.8 m/s, has a  $22.5^\circ$  resolution and  $\pm 3^\circ$  accuracy. It features automatic temperature compensation and operates in a temperature range of  $-20^\circ C$  to  $+85^\circ C$ . The sensor has a working voltage of 12 30VDC, and its output is a 4-20 mA signal.

## 3.4. Servo motors

Two servo motors are required: one for controlling the mainsail, and the other for controlling the rudder. The decision was made to use the preinstalled servo motors as the vessel was

designed operate with these specific servo motors, it also keeps system design costs low. The manual specifies that a metal geared servo is used for rudder control and a sail winch servo is used to control the sail position. Aside from this, no other information is given in the manual about the servo motors.

## 3.5. GPS receiver

The GPS receiver is used to determine the GPS coordinates and speed of the sailing vessel. GPS coordinates of the vessel are needed to calculate the reference bearing (used in rudder control), which is the bearing between current position and the target position. All GPS receivers on the market are accurate to within 2.5m, component choice is therefore dependant on factors such as price, power consumption and update rate. The GPS receiver that is used is a ATGM336H-5N [?] module. It was chosen because it has a high tracking sensitivity, low power consumption and is low cost. Supply voltage of the receiver is 3.3V and it communicates via a UART interface. It has a tracking sensitivity of -162dBm, consumes  $< 25mA$  during continuous operation, has a first positioning time of 32 seconds, maximum update rate of 10Hz, and also features built in antenna short circuit protection.

## 3.6. Digital compass

The digital compass is used to determine the bearing of the sailing vessel, which is compared to the reference bearing to determine if the vessel is off course. It is required that the compass be able to perform tilt compensation, as the vessel will not always be on a level surface out at sea. The error in heading that occurs when tilt compensation has not been implemented is illustrated in Fig.??, where it can be seen that as the pitch angle of the vessel increases, a greater error in heading occurs [?]. To perform tilt compensation a magnetometer is needed to determine magnetic field vector, and a accelerometer is needed to determine the acceleration due to gravity vector. An IMU is a device that contains both a 3-axis magnetometer, 3-axis accelerometer and 3-axis gyroscope. The two options that were considered were a AltIMU-10-V4 [?] made by Pololu Electronics and a MPU-9250/6500 9-axis IMU [?]. Both options feature 16-bit ADC with signal conditioning. The Alt-IMU-10-V4 also features a digital barometer which is not needed for the purposes of this project. The MPU-9250/6500 was chosen for its low cost when compared to the AltIMU-10-V4. The MPU-9250/6500 has a supply voltage of 3.3V, an operating current of 3.5mA and an  $I^2C$  interface.

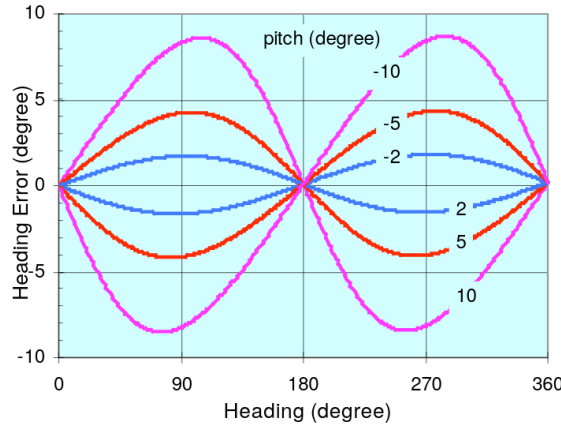


**Figure 3.2:** Heading error due to tilt without tilt compensation [?]

## 3.7. Micro-SD card

The Micro-SD card is used for data-logging purposes, it allows for data from tests to be stored and analysed at a later time. Data that is logged during water tests include: current position, current bearing, desired bearing, bearing error, distance to target, wind direction, and tracking speed. A micro-Sd card socket made by Pololu [?] was used, and features a SPI.

## 3.8. Power system

The power system consists of three separate power sources. The rudder servo and sail winch servo are powered by a 6v battery source consisting of four 1.5V alkaline batteries in series. The Adafruit feather is powered by a 5000mAh 3.7V lithium polymer battery. The Adafruit feather is used to power the micro-SD card socket, GPS receiver, and digital compass. The wind direction sensor is powered with two 9V alkaline batteries in series. The use of one 12V power source with a 3.3V regulator was initially considered. Three separate power sources were chosen because the power consumption of the system is such that two 9V alkaline batteries would only power the system for 2.13 hours, which was considered insufficient.

## 3.9. Metrics

### Data logging

To verify the system is capable of logging data as well as test the successful operation of the GPS receiver, a simple test is conducted. The experimental setup is as follows: The system is carried along a path, the GPS receiver will take samples at a rate of 1Hz, the

GPS coordinates will then be logged to the micro-SD card on each sample, results are then analyzed to determine if path that was logged corresponds to the actual path travelled.

### Digital compass

Successful operation and accuracy of the digital compass is determined with two separate tests.

The first test is done to test the accuracy of the digital compass. The setup is as follows: the digital compass undergoes extensive calibration; the digital compass as well as a handheld magnetic compass shown in Fig. ??, are placed on a level piece of wood and spaced such that they do not interfere with each other; the wood is rotated in steps of  $10^\circ$  anti-clockwise; each step readings from the handheld compass and the digital compass are taken and compared; because of the slight sample deviation present in the digital compass, an average of 10 samples are taken for each step.

The second test is done to determine the successful operation of the tilt compensation algorithm that is used. The setup is the same as the first test, but this time a pitch angle of  $10^\circ$  is applied to the digital compass, the handheld compass is still placed flat. Again the wood is rotated in steps of  $10^\circ$  anti-clockwise, and again ten samples are taken from the digital compass on each step, the average of these samples is used for comparison. The results of this test are compared with the results from the first test - where the digital compass had a pitch and roll angle of zero.

Accuracy of the digital compass needs to be compared with that of the GPS receiver. If the GPS receiver is capable of determining the bearing with better/or even the same degree of accuracy as that of the digital compass, then the use of a digital compass in the system does not make sense. It should be noted that the GPS receiver is only capable of determining bearing when the velocity of the system is greater than zero. The test done to compare the accuracy of these two components is as follows: The GPS receiver is carried along a path of constant bearing and with a velocity similar to that of the maximum velocity the sailboat is capable of, bearing samples are then taken at a frequency of 1Hz, the same is then done for the digital compass, digital compass is held such that it points to the end point of the path throughout the test. The digital compass must be calibrated before the test. The results of the two tests are then compared.

### Navigational calculations

The successful operation of the algorithm used to determine distance between two points is verified using the following experimental setup: a target GPS coordinate is given to the system, the current GPS coordinates are obtained from the GPS receiver at varying distances from the target and distance is calculated, distances that samples are taken are physically measured out before the test is done, an average of ten distance calculations

are done for each change in distance.

### Sail control

A test will be conducted to verify accuracy as well as successful operation of the sail control system. The experimental setup is as follows: wind direction sensor will be adjusted in  $22.5^\circ$  increments - wind sensor's resolution - with  $0^\circ$  corresponding to center on no sail-zone, corresponding change in sail position will then be measured from the centerline of the boat.

### Rudder control

The first test will test the operation of the rudder control out of the water. A target GPS coordinate will be chosen and given to the system, the system will then be carried along a path of constant bearing ending in the target coordinate, the current position, desired bearing, actual bearing and error signal will be logged throughout the test.

The second test will be done on the dam by the Maties canoe club. The experimental setup is as follows: a target coordinate is programmed into the system, the digital compass is calibrated and the sailboat is placed at a suitable starting location. Apparent wind is determined beforehand and the sail position is set accordingly (sail position control will be disabled for this test). The data that will be logged throughout the test is: current GPS coordinate, distance to target, desired heading, actual heading, heading error signal, rudder PWM value and apparent wind direction. The purpose of this test is to evaluate the performance of the rudder controller and determine optimal gains through experimentation, this test will therefore be repeated more than once.

### System

A similar test will be done on water at the Maties canoe club to verify the successful operation of the entire system - navigational and control systems. The test is similar to the second test done for the rudder control except the sail control will be included, and the setup is as follows: a target coordinate is programmed into the system and the digital compass is calibrated, the sailboat is placed at a suitable starting point, data will be logged throughout the test. The data that is logged is: current GPS coordinate, distance to target, desired bearing, actual bearing, bearing error signal, rudder servo PWM value, apparent wind direction, sail position value, sail servo PWM value.

The final test will have the same experimental setup as the previous test, only difference being that two separate waypoints will be set beforehand. This test is done to verify the vessels ability to navigate to a single waypoint and then change navigation to a different waypoint.

# **Chapter 4**

## **Detail Designs**

### **4.1. Micro-controller**

The Adafruit STM32F405 feather has a supply voltage of 3.7V and consumes up to  $80mA$  when operational, it is powered by a 5000mAh 3.7V lithium polymer battery connected with a jst connection. The board features a 3.3V regulator which is to regulate the battery power, there are also pins to distribute the 3.3V regulated power off-board. The 3.3V regulator is used to power the GPS receiver, MPU-9250/6500 IMU, and the micro-SD socket. The board has a USB-C female connector which is used to load the main program and for debugging during the design process. The board is capable of running circuit python, which was used in the development of this project.

### **4.2. GPS receiver**

The GPS receiver has a power supply voltage of 3.3V and is powered by the Feathers 3.3V regulator. It is connected to a pin on the feather which is configured as UART, with a BAUD rate of 9600. The GPS receiver continually receives data at a frequency which is set during the configuration process, in this case its every second. Data sent by the GPS receiver is in the form of ASCII encoded sentences which follow the NMEA protocol [?]. The NMEA protocol defines a number of ASCII identifiers which occur at the beginning of each ASCII sentence, they are used to identify the type of data contained in the sentence. Table ?? shows the specific NMEA sentences which are relevant to this project and their corresponding ASCII identifiers.

### **4.3. Wind Direction Sensor**

The wind direction sensor has a supply voltage in the range 12-30VDC, and is powered by two 9V alkaline batteries in series. It is mounted on the bow of the vessel. It outputs a  $4 - 20mA$  analog signal, which is connected directly to pin A4 of the Feather. Pin A4 on the Feather connects to a 5V tolerant pin on the STM32F405 micro-controller. This pin

**Table 4.1:** NMEA sentence information

Sentence identifier	Description
\$GPGGA	Global Positioning System Fix Data (Time, Latitude, Longitude)
\$GPGLL	Geographic Position, Latitude / Longitude and time.
\$GPGSV	GPS Satellites in view
\$GPVTG	Track Made Good and Ground Speed.
\$GPRMC	Recommended minimum specific GPS/Transit data (Latitude, Longitude, Speed over ground in knots, Track angle made true, Magnetic variation)

was configured to use one of the micro-controllers 12-bit ADC, which has a sampling range of 0V to 3.3V. A shunt resistor with a value of  $160\Omega$  is connected to the sensor output. This value was calculated to produce a voltage over the resister in the range of 642mV to 3.2V. The Actual voltage range measured over the shunt resister was 642mV to 3.07V.

All pins on the STM32F405 micro-controller are capable of sinking or sourcing 25mA maximum, there is therefore no chance of the sensor damaging the micro-controller pin. A digital buffer was initially considered to prevent the micro-controller from loading the sensor output circuit, but was not used as the ADC inputs are high impedance. The STM32F405 data sheet [?] specifies that for an ADC input, the max external impedance allowed for an error below 1/4 of the LSB is  $50K\Omega$ . The shunt resistors value is multitudes smaller than this.

## 4.4. Servo Motors

Both the rudder servo motor and the sail servo winch are powered by a 6V source consisting of four 1.5V alkaline batteries. The rudder servo motor is connected to pin A2 of the feather, the Sail winch servo motor is connected to pin D9 of the Feather. Both these pins are configured to output a 50HZ PWM signal, with a duty cycle set by the rudder and sail position controllers. The rudder angle is measured from the centre line of the boat, this corresponds to the neutral position of the rudder. Positive rudder angle is measured from neutral position to the starboard side of the vessel, negative rudder angle is measured from the neutral position to port side of the vessel. Sail position is measured in degrees from the centre line of the vessel to either the port or starboard side. The maximum and minimum PWM values for both servo motors was determined experimentally and is summarized in table ??, along with the corresponding angles. Note that the sail position minimum angle is  $10^\circ$ , this is in accordance with the recommendations outlined in the sailboats manual.

**Table 4.2:** Servo motor PWM limits

Servo motor	PWM_Min	PWM_Min corresponding angle	PWM_Max	PWM_Max corresponding angle
Rudder	48	60°	102	-60°
Sail	75	10°	120	80°

## 4.5. Micro-SD card

The micro-SD card socket has a supply voltage of 3.3V and is powered with the Feathers 3.3V regulator. It is connected to the Feather using a SPI interface. The micro-SD card sockets MOSI, MISO, and clock lines are connected directly to the corresponding pins on the Feather, the chip select line is connected to pin 6 of the Feather. The micro-SD card is formatted with the FAT32 file system, and as, such writing to the micro-SD card is done with FAT32 protocol.

## 4.6. Digital compass

The MPU-9250/6500 IMU has a supply voltage of 3.3V and is powered by the Feather boards 3.3V regulator. It is connected to the Feather via a  $I^2C$  connection. The IMU has an address pin which is grounded. The purpose of the address pin is for setting the LSB of the  $I^2C$ , this allows two IMU's to be connected to the same bus, which is not needed in this case.

### 4.6.1. Tilt Compensation

To perform tilt compensation, firstly pitch and roll angles of the inertial frame of the vessel must be found. Eq. ?? is used to transform a sampled acceleration vector back to the NED frame of reference, where there exists only a z-component with magnitude  $9.81 \text{ m/s}^2$ . In this equation  $\mathbf{A}_s$  represents the acceleration vector which has been sampled from the IMU,  $g$  is acceleration due to gravity and  $\mathbf{R}_{x,\phi}$ ,  $\mathbf{R}_{y,\theta}$ ,  $\mathbf{R}_{z,\psi}$  represent equations ??, ??, ?? respectively.

$$\mathbf{R}_{y,\theta} \cdot \mathbf{R}_{x,\phi} \cdot \mathbf{A}_s = [0 \ 0 \ g]^T \quad (4.1)$$

Expanding Eq. ??, gives Eq. ???. The components of the sampled acceleration vector are  $A_{sx}$ ,  $A_{sy}$  and  $A_{sz}$ .

$$\begin{bmatrix} \cos\theta & 0 & \sin\theta \\ 0 & 1 & 0 \\ -\sin\theta & 0 & \cos\theta \end{bmatrix} \begin{bmatrix} 1 & 0 & 0 \\ 0 & \cos\phi & -\sin\phi \\ 0 & \sin\phi & \cos\phi \end{bmatrix} \begin{bmatrix} A_{sx} \\ A_{sy} \\ A_{sz} \end{bmatrix} = \begin{bmatrix} 0 \\ 0 \\ g \end{bmatrix} \quad (4.2)$$

Expanding Eq.?? further gives Eq.??, then Eq. ?? and ??.

$$\begin{bmatrix} \cos\theta & \sin\theta\sin\phi & \sin\theta\cos\phi \\ 0 & \cos\phi & -\sin\phi \\ -\sin\theta & \cos\theta\sin\phi & \cos\theta\cos\phi \end{bmatrix} \begin{bmatrix} A_{sx} \\ A_{sy} \\ A_{sz} \end{bmatrix} = \begin{bmatrix} 0 \\ 0 \\ g \end{bmatrix} \quad (4.3)$$

$$A_{s,x}\cos\theta + A_{s,y}\sin\theta\sin\phi + A_{s,z}\sin\theta\cos\phi = 0 \quad (4.4)$$

$$A_{s,y}\cos\phi - A_{s,z}\sin\phi = 0 \quad (4.5)$$

Roll angle  $\phi$  can be found using Eq.?? which results from rearranging terms in Eq.??

$$\phi = \arctan\left(\frac{A_{s,y}}{A_{s,z}}\right) \quad (4.6)$$

By substituting roll angle  $\phi$  into Eq.?? - which is derived from Eq.?? - pitch angle  $\theta$  is found.

$$\theta = \arctan\left(\frac{-A_{s,x}}{A_{s,y}\sin\phi + A_{s,z}\cos\phi}\right) \quad (4.7)$$

Now that pitch and roll angles of the inertial frame of the vessel are known, a sampled magnetometer vector -  $\mathbf{B}_s$  - can be transformed to the NED frame of reference. This is done using Eq.??, where  $\mathbf{B}_r$  is the transformed vector. Eq.?? is not used here as this will eliminate yaw angle  $\psi$  which is needed to determine the resulting bearing

$$\mathbf{B}_r = \mathbf{R}_{y,\theta} \cdot \mathbf{R}_{x,\phi} \cdot \mathbf{B}_s \quad (4.8)$$

Eq.?? is then expanded, giving Eq.?? and Eq.??.

$$\begin{bmatrix} B_{r,x} \\ B_{r,y} \\ B_{r,z} \end{bmatrix} = \begin{bmatrix} \cos\theta & 0 & \sin\theta \\ 0 & 1 & 0 \\ -\sin\theta & 0 & \cos\theta \end{bmatrix} \begin{bmatrix} 1 & 0 & 0 \\ 0 & \cos\phi & -\sin\phi \\ 0 & \sin\phi & \cos\phi \end{bmatrix} \begin{bmatrix} B_{s,x} \\ B_{s,y} \\ B_{s,z} \end{bmatrix} \quad (4.9)$$

$$\begin{bmatrix} B_{r,x} \\ B_{r,y} \\ B_{r,z} \end{bmatrix} = \begin{bmatrix} B_{s,x}\cos\theta + B_{s,y}\sin\theta\sin\phi + B_{s,z}\sin\theta\cos\phi \\ 0 + B_{s,y}\cos\phi - B_{s,z}\sin\phi \\ -B_{s,x}\sin\theta + B_{s,y}\cos\theta\sin\phi + B_{s,z}\cos\theta\cos\phi \end{bmatrix} \quad (4.10)$$

Eq.?? is now derived using Eq.??, where yaw angle  $\psi$  represents the tilt compensated heading of the vessel. The ATAN2() function in python is used to determine the yaw angle, it returns a value in the range of  $-180^\circ$  to  $180^\circ$ . The following check is therefore done in software: if the yaw angle is negative then  $360^\circ$  is added to it. This ensures bearing is in

the range  $0^\circ$  to  $360^\circ$ .

$$\psi = \left( \frac{-B_{r,y}}{B_{r,x}} \right) = \arctan \left( \frac{B_{s,z} \sin \phi - B_{s,y} \cos \phi}{B_{s,x} \cos \theta + B_{s,y} \sin \theta \sin \phi + B_{s,z} \sin \theta \cos \phi} \right) \quad (4.11)$$

#### 4.6.2. Calibration

As mentioned in sec.??, the earth's magnetic field varies in strength and orientation depending on location, ferrous metals nearby the digital compass can also distort the local magnetic field (this could be interference from other components), the digital compass therefore needs to be calibrated to compensate for this. Two disturbances in the earth's magnetic field are compensated for during a calibration process, they include: hard-iron effects and soft-iron disturbances. Hard-iron effects adds a constant magnitude field component along each axis of the sampled magnetic field values. Soft-iron disturbances arise from interaction of the earth's magnetic field, the amount of distortion varies depending on the orientation of the digital compass.

The calibration process is done by rotating the digital compass in such a manner that every axis aligns with all other axes at least once, while this is done, samples from the magnetometer are taken. The maximum and minimum values found along each axis during this process are stored. Eq.?? and Eq.?? are used to determine hard-iron offsets and soft iron values for each axis respectively. After the calibration process has concluded, hard-iron offset is subtracted and soft-iron correction is applied to every sampled value. Eq.?? shows how this is done.

$$\begin{bmatrix} offset_x \\ offset_y \\ offset_z \end{bmatrix} = \begin{bmatrix} \frac{(max_x + min_x)}{2} \\ \frac{(max_y + min_y)}{2} \\ \frac{(max_z + min_z)}{2} \end{bmatrix} \quad (4.12)$$

$$\begin{bmatrix} \delta_x \\ \delta_y \\ \delta_z \end{bmatrix} = \begin{bmatrix} \frac{(max_x - min_x)}{2} \\ \frac{(max_y - min_y)}{2} \\ \frac{(max_z - min_z)}{2} \end{bmatrix} \quad (4.13)$$

$$\delta_{avg} = \frac{(\delta_x + \delta_y + \delta_z)}{3} \quad (4.14)$$

$$\begin{bmatrix} scale_x \\ scale_y \\ scale_z \end{bmatrix} = \begin{bmatrix} \frac{\delta_{avg}}{\delta_x} \\ \frac{\delta_{avg}}{\delta_y} \\ \frac{\delta_{avg}}{\delta_z} \end{bmatrix} \quad (4.15)$$

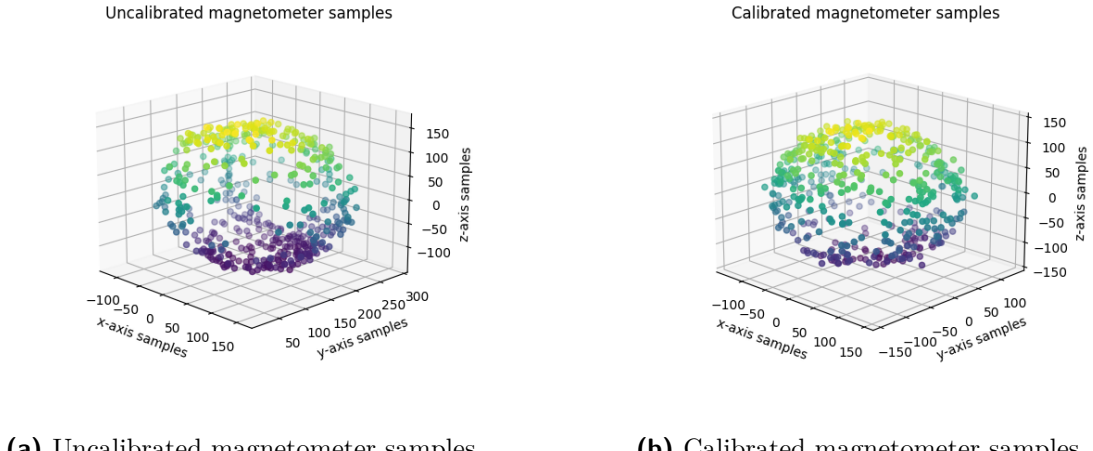


**Figure 4.1:** Calibration process

$$\begin{bmatrix} calibrated_x \\ calibrated_y \\ calibrated_z \end{bmatrix} = \left( \begin{bmatrix} B_{s,x} \\ B_{s,y} \\ B_{s,z} \end{bmatrix} - \begin{bmatrix} offset_x \\ offset_y \\ offset_z \end{bmatrix} \right) \cdot \begin{bmatrix} scale_x \\ scale_y \\ scale_z \end{bmatrix} \quad (4.16)$$

The effects of the calibration process on sampled values is illustrated in Fig.???. Fig.?? is the sampled values taken during a calibration process, the constant offset along each axis caused by hard-iron effects can be seen, soft iron disturbances cause the resulting samples to be ellipsoidal as apposed to spherical. Fig.?? illustrates samples that have been taken after calibration parameters have identified and applied to the samples, it can be seen that the hard-iron offsets have been removed and the soft-iron correction has ensured that the samples taken are approximately spherical in shape.

### 4.6.3. Digital filter

After calibrating the digital compass and applying tilt-compensation, measurement noise was found to be present on the samples taken. A discrete second order Butterworth LPF was thus implemented to reduce the measurement noise. The filter parameters were determined using Scipy.signal.butter(), in Python. Different cutt-off frequencies for the filter were experimented with, the cutt-off frequency that produced minimal deviation on the output of the signal, as well as sufficiently low response time to a step input was chosen.

Five hundred samples were taken with at a sample period of 70 ms, the digital compass was placed on a flat surface with a heading of 90° (verified by the handheld magnetic compass). The mean value of the samples was 89.634°, and variation from the mean was found to be 7.747°. To determine the optimal cutt-off frequency of the LPF filter, the filter was applied to the samples, each time with a different cutt-off frequency, and the resulting deviation at the output was measured. To determine the response time of the

filter to varying cutt-off frequencies, five hundred samples were again taken, but this time the digital compass was rotated  $90^\circ$  during sampling to produce a step input for the filter, response times were then measured to this step input. The resulting deviation at the output and response times for the varying cutt-off frequencies is shown in table???. The cutt-off frequency is shown in the discrete domain, therefore to determine the corresponding frequency in the continuous time domain simply multiply by the sampling frequency, which is 14.286 Hz.

**Table 4.3:** Response time and deviation for different LPF cutt-off frequencies

Cutt-off frequency	Response time (ms)	Variance (degrees)
0.3	137	4.0512
0.25	161	3.4841
0.2	234	2.9346
0.15	363	2.3633
0.12	492	2.1912
0.1	630	1.7741
0.05	1282	1.0558

A cutt-off frequency of 0.12 rad/sample was chosen as it corresponds to a response time of under 500 ms, and a sufficiently low deviation on the output. Fast response time is important in this specific application in order to correct the heading of the vessel quickly, should it go off course.

The transfer function of a discrete second-order Butterworth LPF is shown in Eq.???. The parameters found for a cutt-off frequency of 0.12 rad/sample are shown in Eq.?? and Eq.??

$$Y(z) = \left( \frac{b_0 + b_1 z^{-1} + b_2 z^{-2}}{a_0 + a_1 z^{-1} + a_2 z^{-2}} \right) \cdot X(z) \quad (4.17)$$

$$b = (0.02785977, 0.05571953, 0.02785977) \quad (4.18)$$

$$a = (1., -1.47548044, 0.58691951) \quad (4.19)$$

The LPF filter is then implemented in software as a difference equation shown in Eq.???. The filter was applied to the raw magnetometer and raw accelerometer samples (raw means before tilt-compensation is applied), this was done to avoid a erroneous heading being returned that occurs when samples cross back and forth over  $0^\circ$ . Applying the filter to the accelerometer samples will reduce signal noise caused by high frequency vibrations that occur during a jibe manouvre, due to the sail swapping over.

$$y[n] = \frac{b_0 x[n] + b_1 x[n-1] + b_2 x[n-2] - a_1 y[n-1] - a_2 y[n-2]}{a_0} \quad (4.20)$$

The output of the digital LPF filter designed using a cutt-off frequency of 0.12 rad/sample is shown in Fig.??, and the step response to a  $90^\circ$  step change is shown in Fig.??.



**Figure 4.2:** Discrete LPF output

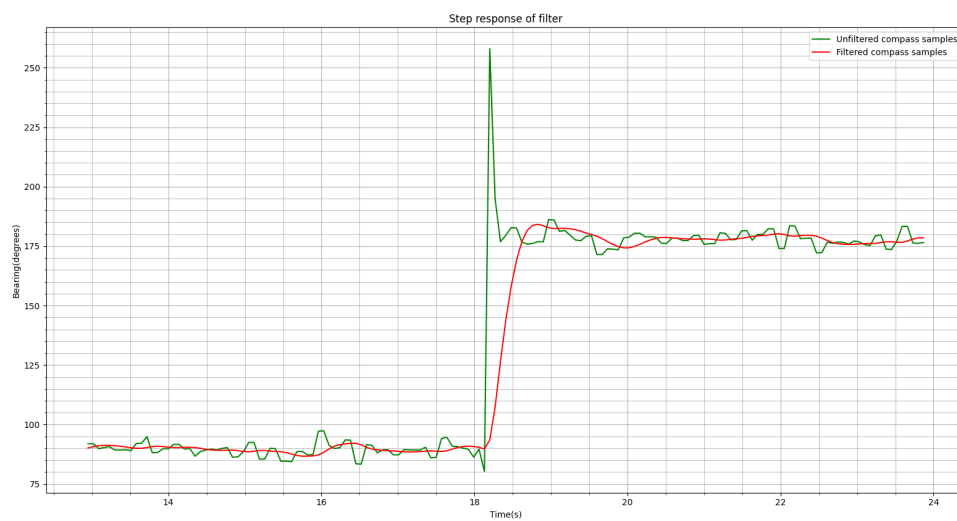


**Figure 4.3:** Discrete LPF step response

## 4.7. Power System

The Adafruit feather consumes a maximum of 80 mA when operating, the MPU-9250/6500 consumes 3.7 mA, the GPS receiver consumes 100 mA and the SD card uses 30 mA

when writing or reading data. The data-sheet for the FST200-202 does not specify power consumption, the maximum current draw was however measured to be 34.2 mA. The overall current draw of the system is therefore 247,9 mA. A 9V Duracell battery has a milli-amp hour capacity of 310 mAh at 100 mA discharge [?]. If two 9V batteries connected in series are used to power the entire system, then the battery life will be less than 1,25 hours. If the two 9V batteries are used to power the wind sensor only, their life will be expanded to roughly 9,064 hours. The decision was therefore made to use the two 9V batteries to power the wind sensor alone, and have a separate power source for the micro-controller, GPS module, digital compass and SD card. A 5000mAh 3.7V lithium polymer battery was used to power the Adafruit feather board. The feathers 3.3V regulator was then used to power the GPS receiver, MPU-9250/6500 IMU and SD card. The Adafruit feathers datasheet specifies that the 3.3V regulator is capable of deliverin 500 mA peak (not continuous) [?]. The combined current draw of the GPS receiver, MPU-9250/6500 IMU and SD card is 133,7 mA, which is much lower than the peak specification. The decision was made to use the power source already present in the RC sailboat to power the two servo motors. The RC sailboat was designed to operate with a 6V power source (four 1.5V alkaline batteries in series) for the two servo motors.

## 4.8. PCB

A printed circuit board was designed using Altium Designer and printed with a LPKF 62 routing machine. The PCB was designed for the Adafruit feather, the GPS receiver, the MPU-9250/6500 and the micro-SD card socket. The PCB has input pins for the 3.7V lithium polymer battery and the 18V power source, the wind sensor connects to the board via a screw terminal and the two servo motors connect to the board with dedicated pins. A power plane was used to distribute ground potential to all the components. The PCB has only one side of copper plating. Component schematics and footprints were made from scratch. Fig.?? shows a schematic of the PCB design, the system diagram used to generate the PCB schematic can be found in appendix??.

## 4.9. Software

### 4.9.1. Control systems

The control systems of the vessel consist of the rudder controller and the sail controller. Fig.?? isllustrates the architecture of the control system. The reference signal for the system is the heading between the current GPS-coordinates and the target GPS-coordinates, the actual heading (measured with the digital compass) is subtracted from the reference heading to create the error signal for the rudder controller. The rudder controller then

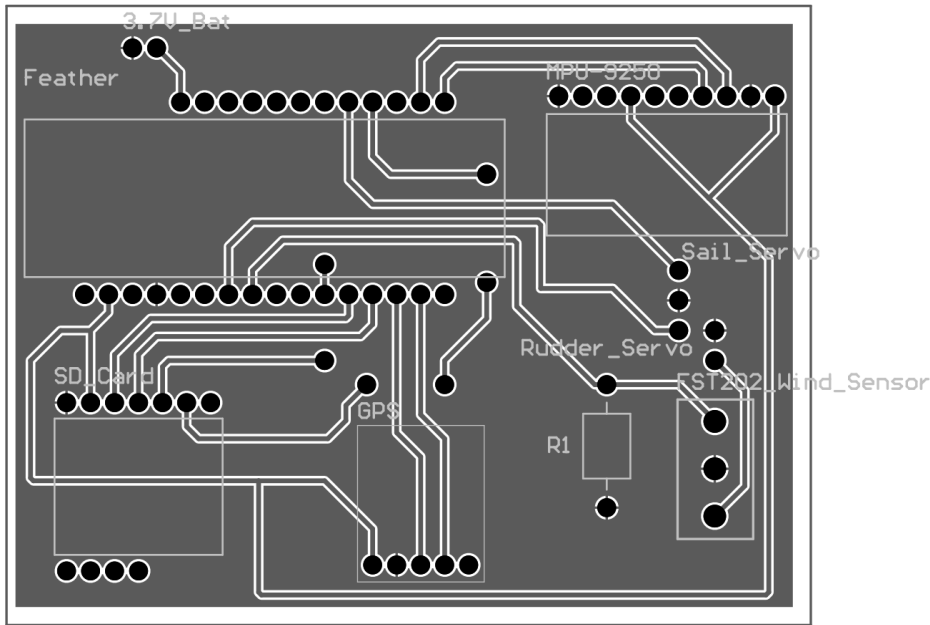


**Figure 4.4:** PCB schematic

controls the rudder actuator (servo motor). The wind direction sensor determines apparent wind direction, this is then input to the sail controller, which adjusts the sail position with a control signal sent to the sail actuator.

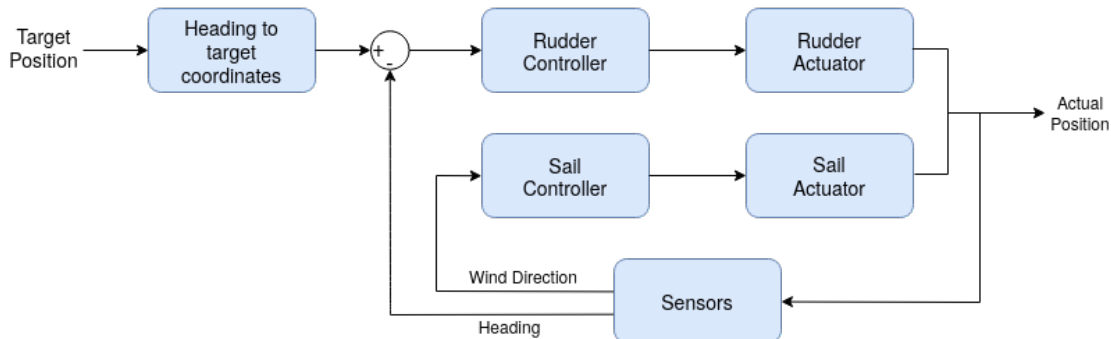


**Figure 4.5:** control system

### Sail controller

The ADC that samples the wind direction sensors output returns a value in the range of 0 to  $2^{16}$ . Table ?? shows the minimum and maximum voltage values measured at the output of the sensor and the corresponding sampled ADC values expressed as a percentage.

Eq.?? is implemented to remove the 642mV offset and convert the sampled ADC value to a value in the range  $0^\circ$  to  $360^\circ$ . This value therefore represents the direction of apparent wind. The cross-over point is the point where the voltage output of the sensor changes from a maximum to a minimum i.e. the voltage drops from 3.07V to 642mV. This drop

**Table 4.4:** Wind direction sensor output limits

	Measured Voltage	ADC sampled value (%)
Minimum	642mV	19.63%
Maximum	3.07V	93.1152%

does not occur instantaneously and because of this erroneous readings can occur if samples are taken at the cross-over point. The controller was therefore designed with the wind sensor orientated such that the cross-over point lies in the no-sail zone, as readings taken in this area are not used anyway.

$$\alpha = \left( \frac{ADC_{sample} - ADC_{min}}{ADC_{max} - ADC_{min}} \right) \cdot 360^\circ \quad (4.21)$$

When designing the sail controller the limits of the sail vessel must be taken into account i.e. the no sail zone. The sail position must be at  $10^\circ$  when the apparent wind is  $\pm 45^\circ$ , and sail position must be at  $80^\circ$  when apparent wind is at  $\pm 180^\circ$ . Eq.?? implements these requirements using PWM maximum and minimum values measured and recorded in table ???. The duty cycle of the PWM signal used for the sail servo winch is stored in a 16 bit register, and is set using Eg.??.

$$PWM_{val} = \left( \frac{\alpha - 45^\circ}{180^\circ - 45^\circ} \right) \cdot (PWM_{max} - PWM_{min}) + PWM_{min} \quad (4.22)$$

$$duty\_cycle = \left( \frac{PWM\_value}{1000} \right) \cdot 2^{16} \quad (4.23)$$

## Rudder Controller

The rudder controller can be designed through simulation, using the methods described in subsection ??, or by adjustment through experimentation. To design a rudder controller using simulation methods, the dynamics of the sail vessel need to be determined, which is not a trivial task. Eq.?? is used to calculate and model the dynamics of a sail vessel, and involves calculating hydrodynamics, moment of inertia, viscous damping, lift, effort sail and centre of mass. From results in subsection ??, it is clear that the controller parameters determined through simulation were not optimal and therefore of design rudder controller for this project is done by adjustment.

The rudder controller used is a proportional controller. The control law for this controller is shown in Eq.??, where  $k_p$  is the proportional gain and  $E_r$  is the error signal. The error signal is determined using Eq.??, where  $\psi_r$  is the reference bearing and  $\psi_a$  is the actual bearing of the vessel.

$$U[k] = k_p E_r \quad (4.24)$$

$$E_r = \psi_r - \psi_a \quad (4.25)$$

After calculating the error signal a check is done in software: if the error signal is greater than  $180^\circ$  then subtract  $360^\circ$ , and if the error signal is smaller than  $180^\circ$  then add  $360^\circ$ , else do nothing. This check is done to ensure that the vessel turns in the direction associated with the smallest angle of correction. For example: if the angle of correction in the clockwise direction is  $100^\circ$  and  $60^\circ$  in the anti-clockwise direction, the boat will turn anti-clockwise.

Eq.?? is used to determine the duty cycle - Eq.?? - of the PWM signal that controls the rudder servo. The maximum and minimum PWM values measured in table ?? are used here.

$$PWM_{val} = \left( \frac{U[k]}{60^\circ} \right) \cdot (PWM_{max} - PWM_{min}) + \left( \frac{PWM_{max} + PWM_{min}}{2} \right) \quad (4.26)$$

## 4.9.2. Navigational calculations

### Distance

To calculate distance over the surface of a sphere two options were considered: The Haversine formulae and the equirectangular approximation. The Haversine formulae is more accurate but can be computationally expensive, the equirectangular approximation is less accurate but more efficient. The Haversine formulae was chosen as the accuracy is required. The Haversine formulae is shown in Eq.?? and Eq.??, where the current coordinates are  $(lat_1, long_1)$  and the target coordinates are  $(lat_2, long_2)$ , R is the radius of the earth in km. Coordinates are in decimal degrees.

$$a = \sin^2 \left( \frac{lat_2 - lat_1}{2} \right) + \cos(lat_1) \cdot \cos(lat_2) \cdot \sin^2 \left( \frac{long_2 - long_1}{2} \right) \quad (4.27)$$

$$d = R \cdot \left( 2 \arctan \left( \frac{\sqrt{a}}{\sqrt{1-a}} \right) \right) \quad (4.28)$$

Eq.?? returns values in the order of  $e - 17$  for a distance on 1m. In Python floats are single precision numbers with a maximum value of  $\pm 3.4e38$  and minimum value of  $\pm 1.7e - 38$ , therefore the haversine function can be used to determine small distances on the micro-controller.

## Heading

To calculate reference heading Eq.?? is used.

$$\psi_r = \arctan \left( \frac{\sin(\text{long}_2 - \text{long}_1) \cos(\text{lat}_2)}{\cos(\text{lat}_1) \sin(\text{lat}_2) - \sin(\text{lat}_1) \cos(\text{lat}_2) \cos(\text{long}_2 - \text{long}_1)} \right) \quad (4.29)$$

### 4.9.3. Program flow

# Chapter 5

## Results

### 5.1. Data logging

The resulting GPS coordinates that were stored to the micro-SD card during the data logging test were plotted on a map of Stellenbosch, and are shown in red in Fig.???. The actual path that was travelled was a loop starting on the corner of Victoria and Ryneveld street, then a left turn onto Bosman street, a left turn onto Merriman avenue and a left turn back onto Ryneveld street.

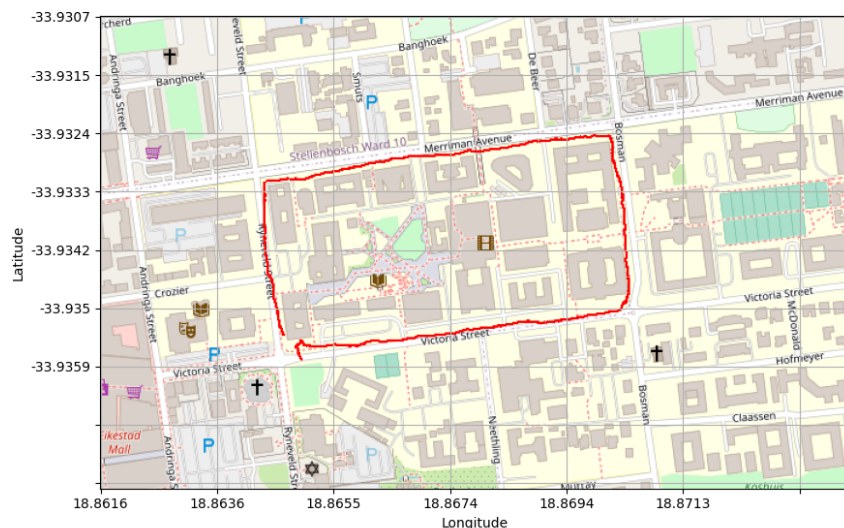


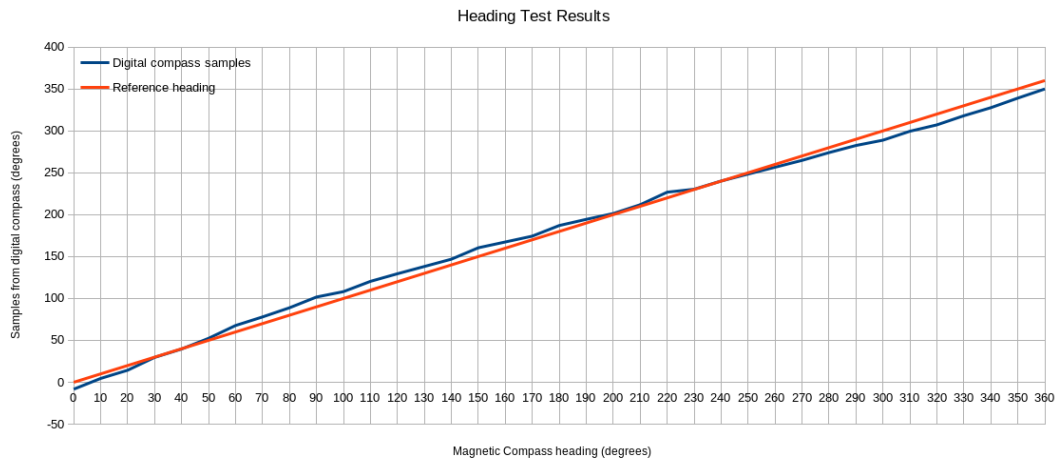
**Figure 5.1:** GPS coordinates of path travelled

The GPS coordinates correspond approximately to the actual path that was travelled,

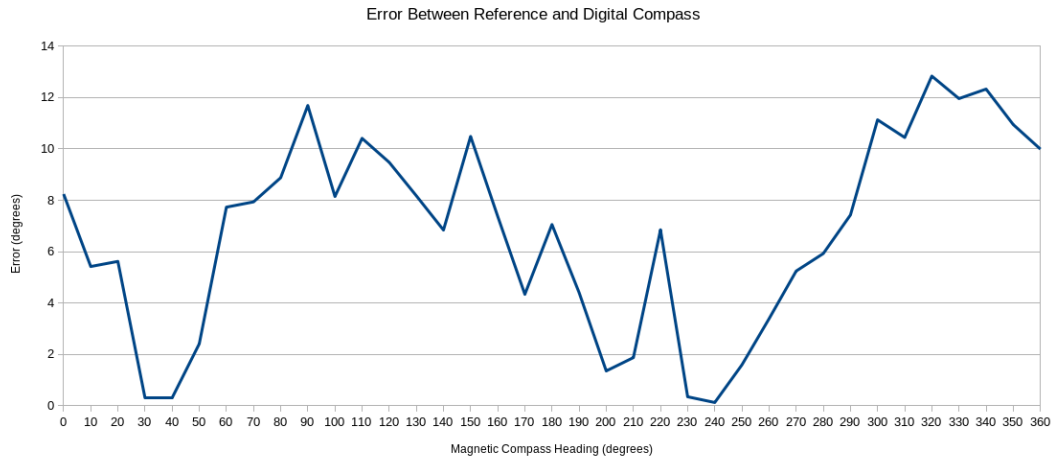
and the accuracy of the GPS receiver is therefore sufficient for the purposes of this project. These results have also verified the data logging capabilities of the system.

## 5.2. Digital Compass

Two separate tests were done to test the accuracy of the digital compass. The results of the first test are shown in Fig.???. The error between the digital compass and the handheld compass is shown in Fig.???. The average error was calculated to be  $6.7312^\circ$ . The error can be attributed to an inadequate calibration process - compass rotation does not cover all possible angles, calibration process too short or sample frequency used not high enough.



(a) Digital compass heading compared to handheld compass heading



(b) Error between Digital compass heading and handheld compass heading

**Figure 5.2:** Digital compass accuracy test

The test was therefore redone, this time an extensive calibration of the digital compass was done. The results of the second test are shown in Fig.???. The error between the digital compass and the handheld compass is shown in Fig.???. The average error for this test was calculated as  $1.5091^\circ$ . The results of this test verify that the digital compass is

accurate when placed on a flat surface.

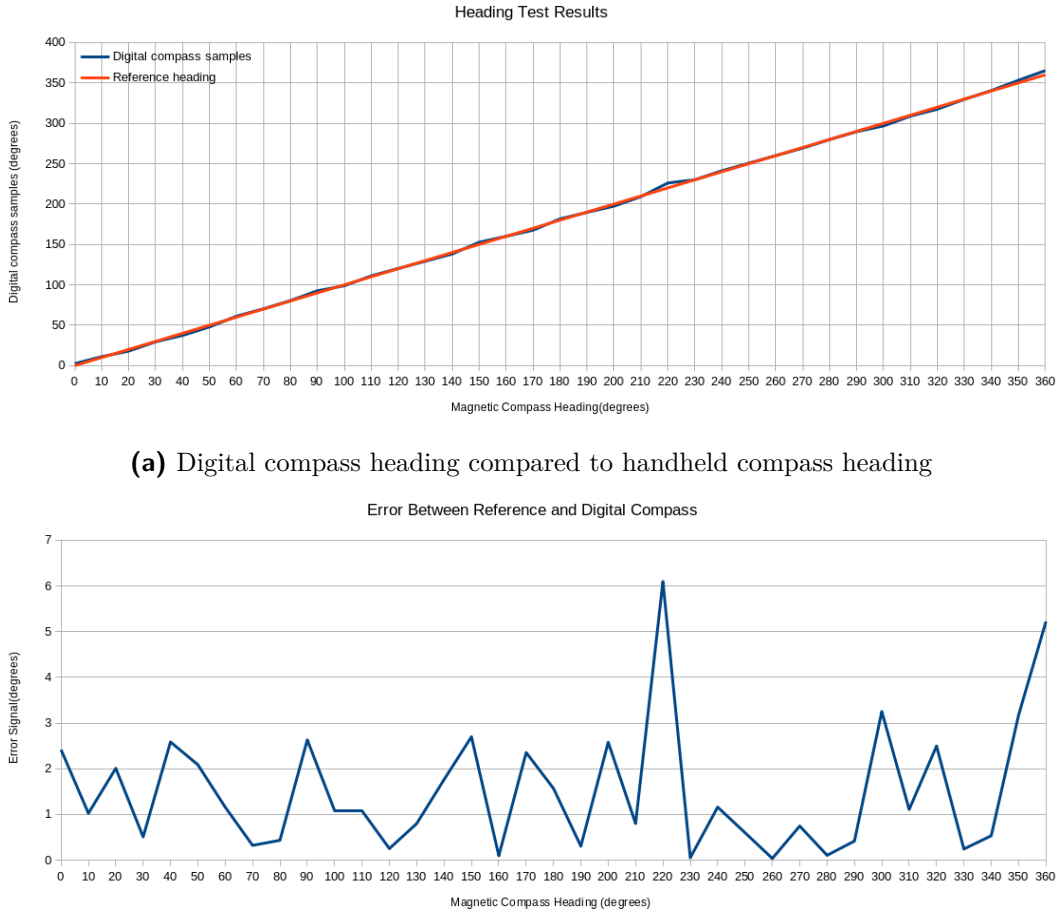
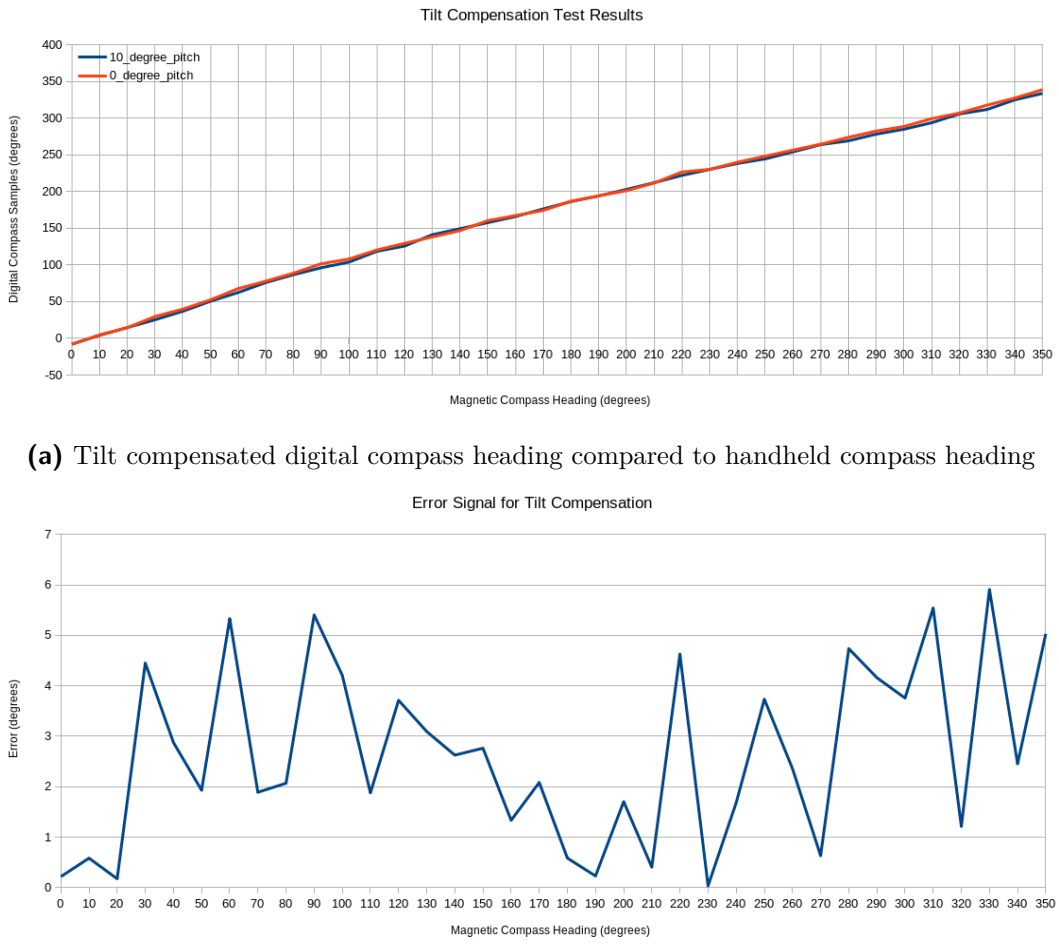


**Figure 5.3:** Digital compass accuracy test

The results of the tilt compensation test are shown in Fig.???. It should be noted that this test was conducted using the same calibration values (hard-iron offset and soft-iron correction values) that were determined and used in Fig.???. The results of the tilt compensation test are therefore compared to the results of the test done in Fig.???

The tilt-compensated digital compass readings are approximately equal to the results obtained when the digital compass had a pitch angle of zero. The error in the results seen in Fig.?? can be attributed to the slight difference in angle when adjusting the wooden platform by hand between the  $10^\circ$  steps. The average error was found to be equal to  $2.6502^\circ$ . The calculations done in section ?? show that the samples taken at varying degrees of pitch angle should theoretically be the same. The results shown in Fig.?? show that the tilt compensation algorithm does work.



(b) Error between tilt compensated digital compass heading and handheld compass heading

**Figure 5.4:** Tilt compensation algorithm test

## 5.3. Sail Control

The first test was done to verify the accuracy of the wind direction measurements, the results are shown in Fig.???. From these results it can be seen that the measured wind direction deviates slightly from the actual direction of the wind vain. The purpose of the wind sensor is to determine the optimal sail position, sail position does not however affect the navigation of the vessel, only the speed of the vessel. Therefore absolute accuracy in measuring wind direction is not of the utmost importance, and deviation in measured results is acceptable.

The second test conducted, measured the change in sail position given a change in apparent wind direction. The results of this test are shown in Fig.???. The resulting measurements closely match the expected results. The sail position is at approximately  $80^\circ$  when the apparent wind is at  $\pm 180^\circ$ , sail position then decreases linearly as the absolute apparent wind value decreases towards  $45^\circ$  - limit of no-sail zone - which corresponds to a sail position of  $10^\circ$ . As expected the sail position stays at  $10^\circ$  for apparent wind in the

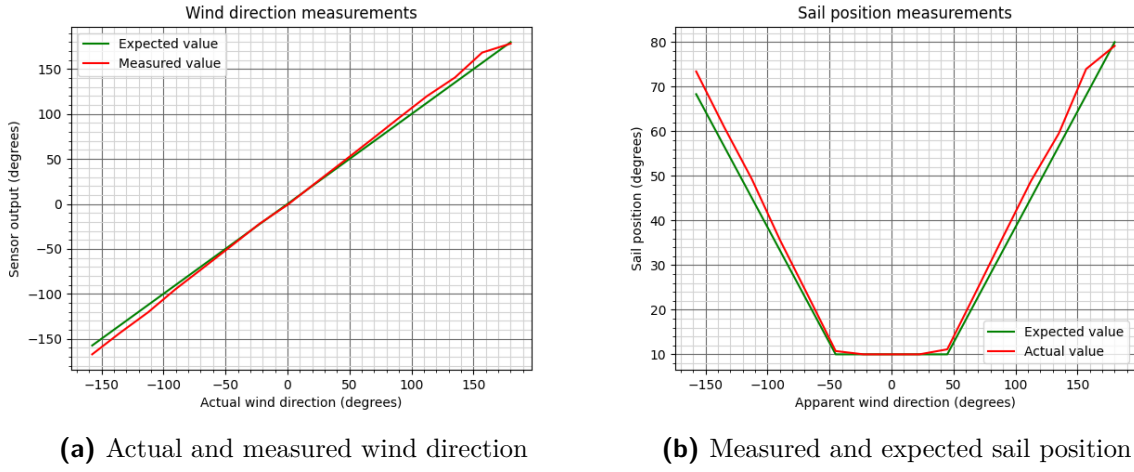


**Figure 5.5:** Sail controller test results

range  $\pm 45^\circ$ .

## 5.4. Rudder control

### 5.4.1. Test-1

The results of the rudder control test which was conducted out of the water are shown in Fig.???. The average value of reference heading is  $44.603^\circ$  and the average value of actual heading is  $44.728^\circ$ . These values are approximately equal and therefore the error signal that is generated for the rudder controller should keep the vessel on course when on water. The variance of the actual heading during the test was calculated as  $13.178^\circ$ , which can be attributed to slight sway when walking.

### 5.4.2. Test-2

For the first rudder control test conducted on the water, the apparent wind was determined before hand to be roughly  $100^\circ$ , the sail position was therefore set to  $40^\circ$ . For this test instead of calculating the reference heading - using the current GPS coordinates and target GPS coordinates - on every iteration a fixed reference bearing was set as  $113^\circ$  beforehand. The proportional gain factor was set to 1.8. The GPS coordinates logged during the test were plotted with Python and are shown in Fig.???

During the test the vessel was visibly oscillating from starboard to port side, this can be seen when analyzing Fig.???, which is a plot of the measured heading and reference heading data, logged throughout the test. The average actual heading value is  $115,404^\circ$  and the variance is  $216,495^\circ$ . The oscillation indicates that the proportional gain factor is too high and overshoot is occurring.

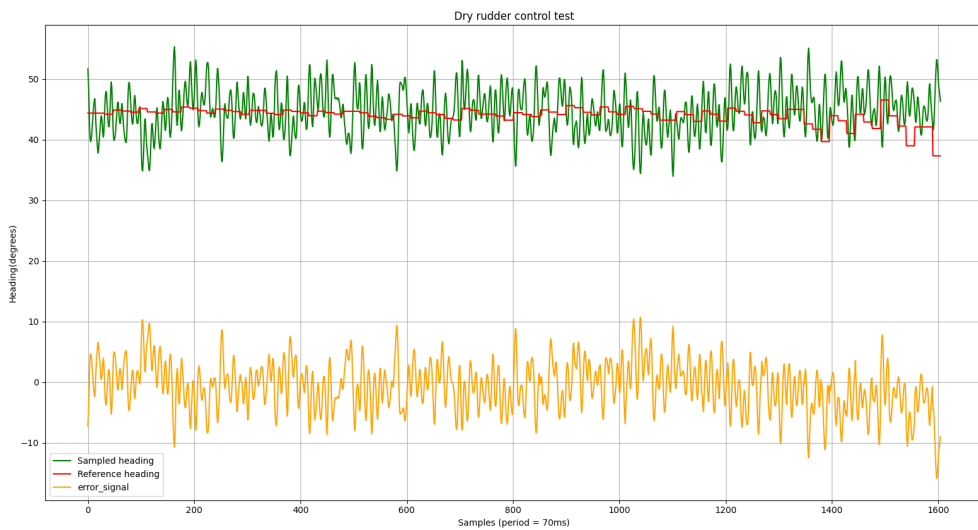


**Figure 5.6:** Results of rudder control test out of water

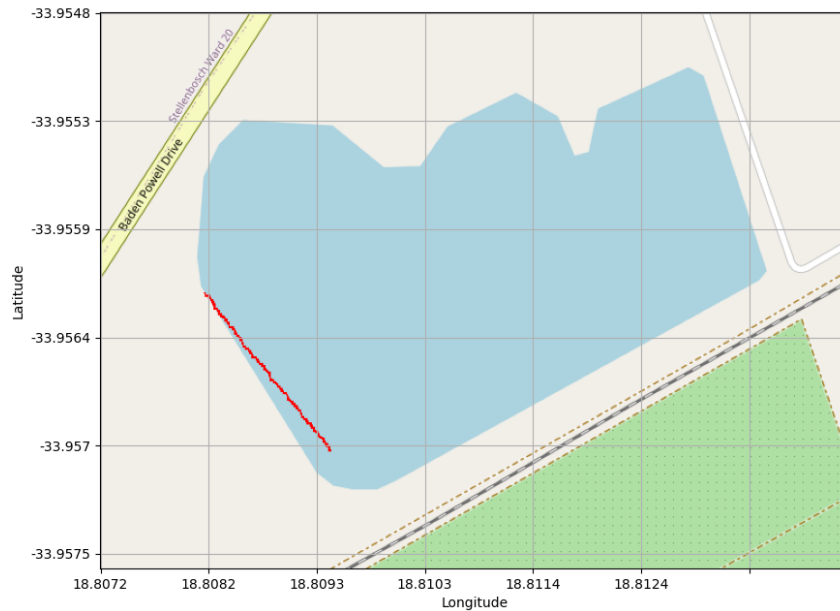


**Figure 5.7:** GPS coordinates of path travelled

The error signal, which is input to the rudder controller is shown in Fig.???. The maximum speed reached during the test was 1.161 knots. Although the sail controller was

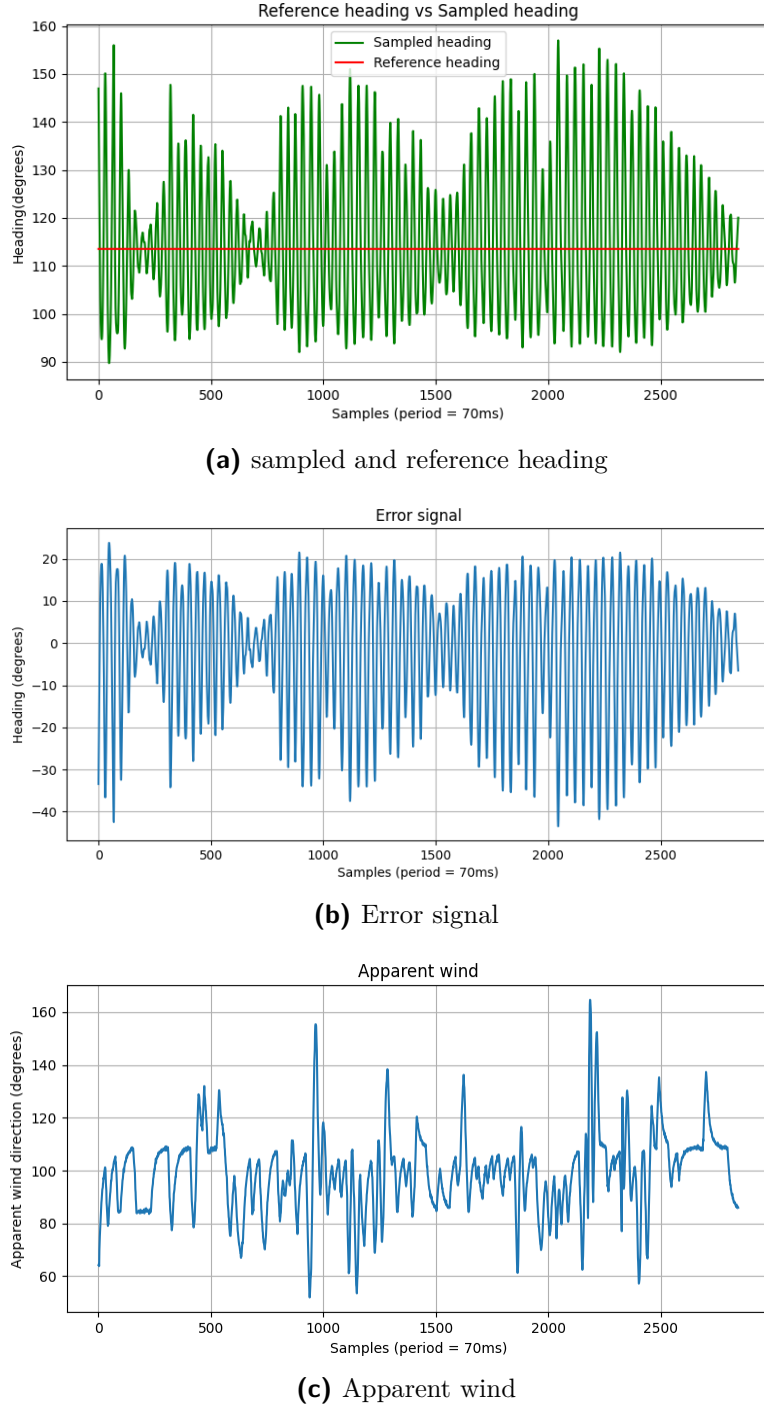


**Figure 5.8:** First rudder control test on water

not implemented during this test, wind direction readings were still taken and the data is illustrated in Fig.???. The average apparent wind value is  $98.8^\circ$ , which corresponds to the initial wind direction reading that was taken. The variation in apparent wind direction throughout the test can be attributed to the oscillating of the vessel.

### 5.4.3. Test-3

Another test was conducted on the water, this time the reference heading was calculated using current and target GPS coordinates after every sampling period. A GPS coordinate corresponding to a point on the side of the dam was set as the target location. The proportional gain factor was set to 1.4. The sail position controller was again not used during this test, instead the apparent wind was measured beforehand. The apparent wind direction was determined to be  $-85^\circ$  and the sail position was set to  $40^\circ$ . The GPS coordinates that were logged throughout the test are shown in Fig.??.

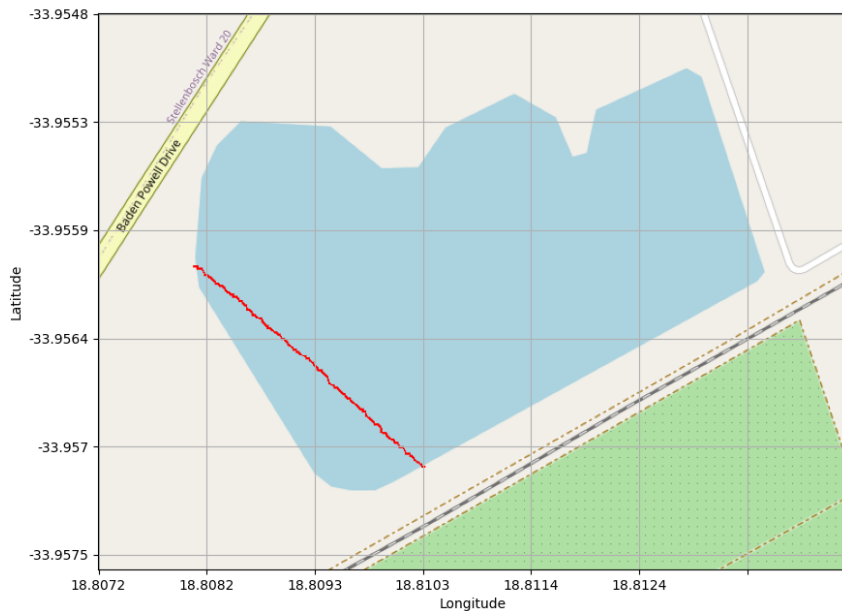


**Figure 5.9:** GPS coordinates of path travelled

The reference and actual bearing values that were logged throughout the test are shown in Fig.???. The error signal that was generated for the rudder controller can be seen in Fig.???. The average of the actual bearing is  $112.32^\circ$  and the variance is  $4.77^\circ$ . The average of the reference heading is  $111.26^\circ$ . The variance of the actual bearing is similar to that of Test-1, the proportional gain value of 1.4 is therefore close to optimal. The difference between the actual and reference heading averages is very slight and the rudder controller therefore tracked the reference signal sufficiently.

Again the apparent wind was logged throughout the test even though the sail controller

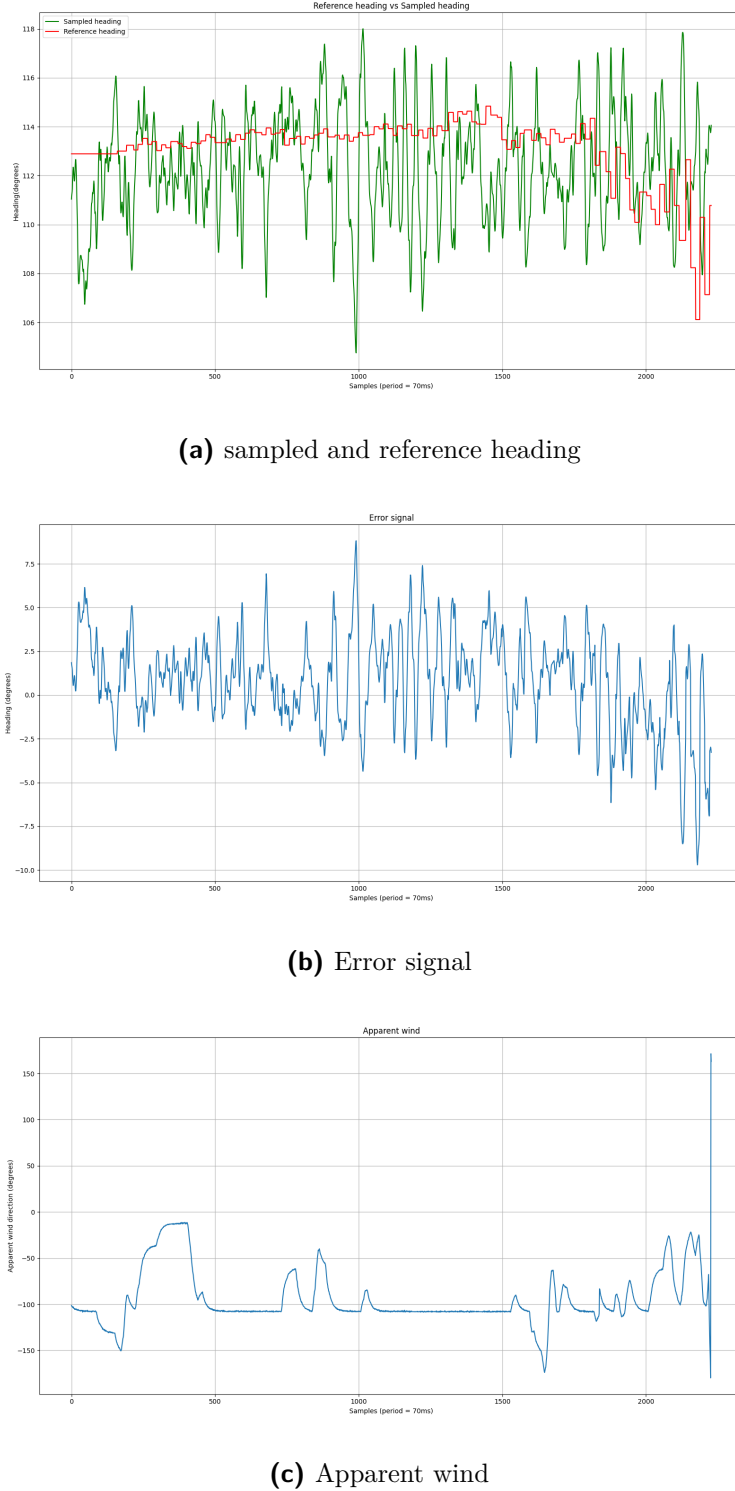


**Figure 5.10:** Second rudder control test on water

was not active, the results are shown in Fig.???. The average apparent wind was calculated to be  $-93.816^\circ$  which is slightly off from the value calculated initially. The apparent wind direction throughout the test appears to be more stable than the results obtained in Test-2, this is due to the vessel maintaining a near constant heading as opposed to the oscillation that occurred in Test-2.

## 5.5. System

### 5.5.1. Test-1

### 5.5.2. Test-2

A test was conducted with two separate waypoints being set beforehand. The first waypoint was the GPS coordinates of a point roughly located in the centre of the dam, the second was that of a point next to the first waypoint, on the shore of the dam. The GPS coordinates logged throughout the test were plotted and are shown in Fig.??.

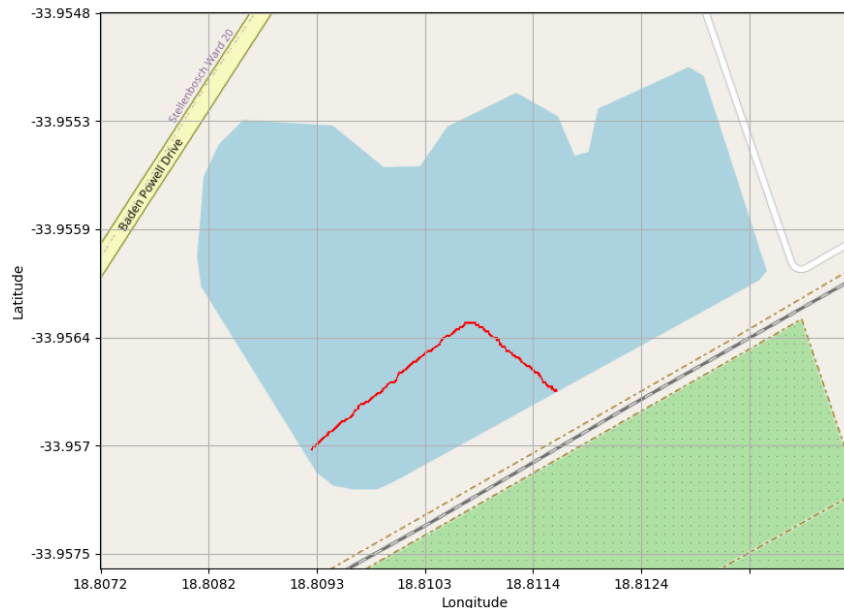
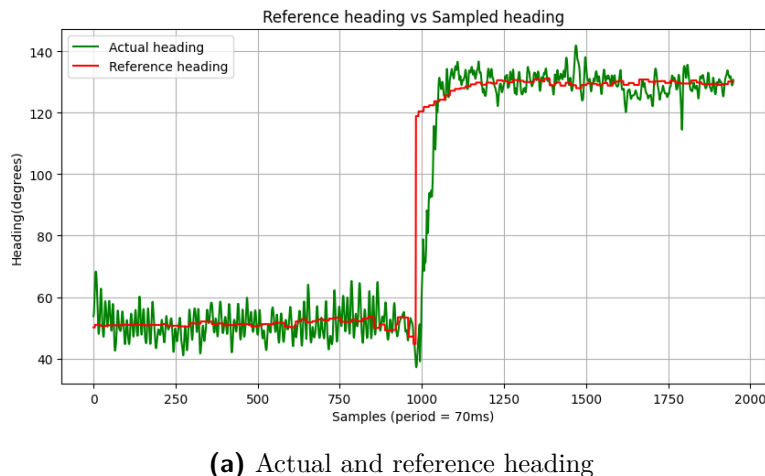


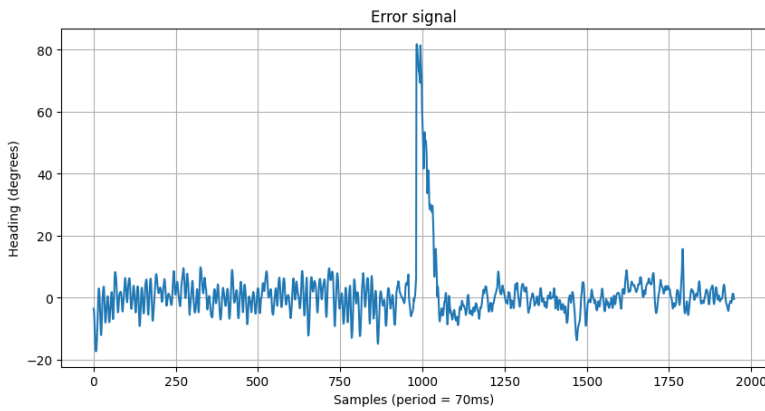
**Figure 5.11:** GPS coordinates of path travelled

The actual and reference heading values logged throughout the test are shown in Fig.???. The error signal that was generated for the rudder controller is shown in Fig.???. The change in heading of the vessel corresponds to a spike with an approximate maximum value of  $80^\circ$  in the error signal. It should be noted that even though the absolute value of the error signal is capable of being larger than  $60^\circ$ , a check is done in software to keep the PWM value within its limits - which correspond to  $\pm 60^\circ$ .

It can be seen that the rudder controller tracked the reference signal sufficiently throughout the duration of the test, even when an approximate step change occurred. The vessel is therefore capable of navigating between multiple waypoints situated outside of the vessels no-sail zone.



(a) Actual and reference heading



(b) Error signal

dam-test-4/wind.png

(c) Apparent wind

**Figure 5.12:** Second system test on water

# **Chapter 6**

## **Summary and Conclusion**

# Appendix A

## System schematic

